

Durham Research Online

Deposited in DRO:

12 January 2015

Version of attached file:

Accepted Version

Peer-review status of attached file:

Peer-reviewed

Citation for published item:

Vernon, R. and Holdsworth, R.E. and Selby, D. and Dempsey, E. and Finlay, A.J. and Fallick, A.E. (2014) 'Structural characteristics and Re–Os dating of quartz-pyrite veins in the Lewisian Gneiss Complex, NW Scotland : evidence of an Early Paleoproterozoic hydrothermal regime during terrane amalgamation.', *Precambrian research.*, 246 . pp. 256-267.

Further information on publisher's website:

<http://dx.doi.org/10.1016/j.precamres.2014.03.007>

Publisher's copyright statement:

NOTICE: this is the author's version of a work that was accepted for publication in *Precambrian Research.*. Changes resulting from the publishing process, such as peer review, editing, corrections, structural formatting, and other quality control mechanisms may not be reflected in this document. Changes may have been made to this work since it was submitted for publication. A definitive version was subsequently published in *Precambrian Research*, 246, June 2014, 10.1016/j.precamres.2014.03.007.

Additional information:

Use policy

The full-text may be used and/or reproduced, and given to third parties in any format or medium, without prior permission or charge, for personal research or study, educational, or not-for-profit purposes provided that:

- a full bibliographic reference is made to the original source
- a [link](#) is made to the metadata record in DRO
- the full-text is not changed in any way

The full-text must not be sold in any format or medium without the formal permission of the copyright holders.

Please consult the [full DRO policy](#) for further details.

1
2 Structural characteristics and Re-Os dating of quartz-pyrite veins in the
3
4 Lewisian Gneiss Complex, NW Scotland: evidence of an Early
5
6
7 Paleoproterozoic hydrothermal regime during terrane amalgamation.
8
9

10
11
12 R. Vernon^{1*}, R.E. Holdsworth^{1†}, D. Selby¹, E. Dempsey¹, A. J. Finlay¹ & A. E. Fallick²
13
14
15

16
17 ¹ *Department of Earth Sciences, Durham University, Durham, DH1 3LE, UK.*
18

19 ² *SUERC, Scottish Enterprise Technology Park, Rankine Avenue, East Kilbride, G75 0QF,*
20
21 *UK.*
22

23 **Current address: Department of Geology, University of Leicester, University Road,*
24
25 *Leicester, LE1 7RH, UK.*
26

27
28 [†]Corresponding author
29
30
31

32 **Abstract:** In the Archaean basement rocks of the Assynt and Gruinard terranes of the
33
34 mainland Lewisian Complex in NW Scotland, a regional suite of quartz-pyrite veins cross-cut
35
36 regional Palaeoproterozoic (Badcallian, ca. 2700 Ma; Inverian, ca. 2480 Ma) fabrics and
37
38 associated Scourie dykes. The quartz veins are overprinted by amphibolite-greenschist
39
40 facies Laxfordian deformation fabrics (ca. 1760 Ma) and later brittle faults. The hydrothermal
41
42 mineral veins comprise a multimodal system of tensile/hybrid hydraulic fractures which are
43
44 inferred to have formed during a regional phase of NW-SE extension. The almost orthogonal
45
46 orientation of the quartz veins (NE-SW) to the Scourie dykes (NW-SE) are incompatible and
47
48 must result from distinct paleostress regimes suggesting they are related to different tectonic
49
50 events. This hypothesis is supported by Rhenium-Osmium dating of pyrite that yields an age
51
52 of 2249 ± 77 Ma, placing the vein-hosted mineralisation event after the oldest published
53
54 dates for the Scourie Dykes (2420 Ma), but before the youngest ages (1990 Ma). Sulphur
55
56 isotope analysis suggests that the sulphur associated with the pyrite is isotopically
57
58
59
60
61
62
63
64
65

1
2
3
4
5
6
7
8
9
10
11
12
13
14
15
16
17
18
19
20
21
22
23
24
25
26
27
28 indistinguishable from primitive mantle. The presence of the ca. 2250 Ma quartz-pyrite veins
29 in both the Assynt and Gruinard terranes confirms that these crustal units were
30 amalgamated during or prior to Inverian deformation. The absence of the veins in the
31 Rhiconich Terrane is consistent with the suggestion that it was not finally amalgamated to
32 the Assynt Terrane until the Laxfordian.
33 **[End]**

34
35
36
37
38
39
40
41
42
43
44
45
46
47
48
49
50
51
52
53
54
55
56
57
58
59
60
61
62
63
64
65

1. Introduction

The Archaean gneisses of the Lewisian Complex in NW Scotland form a well exposed and relatively accessible area of Laurentian continental basement rocks that lie in the immediate foreland region of the Palaeozoic Caledonian Orogen (Fig. 1). Like many regions of continental metamorphic basement, the Lewisian Complex preserves evidence for multiple episodes of igneous intrusion, ductile and brittle deformation together with associated phases of metamorphism and mineralisation (e.g. Sutton and Watson 1951; Park 1970; Beacom et al., 2001; Wheeler et al., 2010). Whilst cross-cutting and overprinting relationships observed in the field and thin section allow *relative* age relationships to be established on both regional and local scales, only radiometric ages are able to give information concerning the absolute timing of events. Despite the emergence of an increasing number of geochronometers for Earth Scientists, an enduring problem in many basement regions is a relative paucity of material suitable for reliable radiometric dating. This lack of absolute age determinations has become a particularly significant problem in the Lewisian Complex since Kinny et al. (2005) and Friend and Kinny (2001) proposed that the Lewisian may comprise a number of lithologically and geochronologically distinct tectonic units or terranes assembled progressively during a series of Precambrian amalgamation episodes perhaps spanning more than a billion years (see Park, 2005; Goodenough et al., 2013 for discussions).

This paper describes the lithology, field relationships and microstructures of a little described set of quartz-pyrite veins that are recognised throughout the Assynt Terrane and within the Gruinard Terrane. These mineralised hydrofractures display a consistent set of contact relationships relative to regionally recognised igneous, metamorphic and deformational events. Rhenium-osmium (Re-Os) geochronology on pyrites collected from these veins is used to obtain a consistent set of ages that better constrain the absolute timing of events in this important part of the Lewisian Complex in NW Scotland. It also illustrates the potential value of the Re-Os technique as a means of dating sulphide mineralisation events in geologically complex continental basement terrains worldwide.

62

63 2. Regional Setting

64 The Precambrian rocks of the Lewisian Complex of NW Scotland form a fragment of the
 65 continental basement of Laurentia that lies to the west of the Caledonian Moine Thrust (Fig.
 66 1). The rocks are for the most part little affected by Caledonian deformation and have
 67 experienced a number of major crustal-scale geological events during the Archaean and
 68 Palaeoproterozoic. The Lewisian Complex is divided into a number of tectonic regions or
 69 terranes which are predominantly separated by steeply-dipping shear zones or faults (e.g.
 70 Park et al., 2002; Park, 2005).

71 The Assynt Terrane (Fig. 1) forms the central part of the Lewisian Complex in
 72 mainland NW Scotland. It comprises grey, banded, tonalite-trondjemite-granodioritic (TTG)
 73 gneisses which are locally highly heterogeneous lithologically, ranging from ultramafic to
 74 acidic compositions (e.g., Sheraton et al., 1973). The TTG gneisses are thought to be
 75 derived from igneous plutons intruded at 3030 to 2960 Ma (high precision U-Pb and Sm-Nd
 76 geochronology; Hamilton et al., 1979; Friend and Kinny, 1995; Kinny and Friend, 1997).
 77 These rocks then underwent deformation and granulite-facies metamorphism during the so-
 78 called Badcallian event(s) which led to significant depletion of large-ion lithophile elements in
 79 the TTG gneisses that is more extensive in the Assynt Terrane compared to adjacent
 80 amphibolite-facies terranes (e.g. Rhiconich, Gruinard; Moorbath et al., 1969; Cameron,
 81 1994; Wheeler et al., 2010). The timing of Badcallian events are incompletely resolved with
 82 current age constraints suggesting either *ca.* 2760 Ma (e.g., Corfu et al.1994; Zhu et al.,
 83 1997), and/or *ca.* 2490 - 2480 Ma (e.g., Friend and Kinny 1995; Kinny & Friend, 1997).

84 The central part of the Assynt Terrane is cut by the major NW-SE-trending, steeply
 85 dipping dextral transpressional Canisp Shear Zone (CSZ) which has a maximum width of
 86 1.5km (Attfield, 1987; Fig. 1). There are also many other smaller steeply-dipping, NW-SE to
 87 WNW-ESE trending minor shear zones cutting the surrounding Badcallian gneisses (Park
 88 and Tarney, 1987). Some of these shear zones, including the CSZ, developed initially during
 89 Inverian deformation and amphibolites-facies retrogression which affected substantial parts

of the Assynt Terrane. The absolute age of this event is the subject of significant uncertainty and debate, with a majority of studies considering it to be *ca.* 2490 - 2480 Ma (e.g., Corfu et al. 1994; Love et al., 2004; Goodenough et al., 2013). Others (e.g., Friend and Kinny 1995; Kinny and Friend, 1997) suggest that the Inverian is a younger – as yet undated – event younger than *ca.* 2480 Ma while still pre-dating the oldest Scourie dykes. These mafic to ultramafic Scourie dykes are found throughout the Assynt Terrane, ranging in thickness from a few mm to several tens of m and were intruded *ca.* 1900 - 2400 Ma (Rb-Sr whole rock and U-Pb geochronology; Chapman 1979; Heaman & Tarney, 1989; Davies & Heaman 2014). The NW-SE-trending Scourie dykes cross-cut local Inverian fabrics and display evidence of having been emplaced under amphibolite facies pressures and temperatures, i.e. in the middle crust, possibly immediately following the Inverian event (O'Hara, 1961; Tarney, 1973; Wheeler et al., 2010).

In the Assynt Terrane, the significantly later main phase Laxfordian event has traditionally been associated with the shearing of the Scourie dykes and widespread retrogression of the TTG gneisses under lower amphibolite to upper greenschist-facies metamorphic conditions (e.g., Sutton and Watson, 1951; Attfield, 1987; Beacom et al., 2001). The Laxfordian is recognised throughout much of the Lewisian complex and appears to be a long lived series of events starting with a series of magmatic events *ca.* 1900-1870 Ma – at least some of which are related to island arc development – followed by a protracted orogenic episode lasting from 1790 - 1660 Ma (see discussion in Goodenough et al., 2013). The effects of Laxfordian reworking in the Assynt Terrane are highly localised, being largely restricted to the central part (*ca.* 1km wide) of the CSZ and other shear zones, as well as along the margins of the Scourie dykes. This contrasts with the neighbouring Rhiconich and Gruinard Terranes where the Laxfordian event reached amphibolite facies and was associated with more pervasive ductile shearing and reworking (Droop et al., 1989). This has led to the suggestion that the Assynt Terrane represents a shallower depth crustal block during the Laxfordian (e.g., Dickinson and Watson, 1976; Coward and Park, 1987).

In the Assynt and Gruinard terranes, a younger set of 'late Laxfordian' sinistral low greenschist-facies mylonitic shear zones, brittle faults and localized folds is recognised developed sub-parallel to the pre-existing high-strain fabrics in Laxfordian and Inverian shear zones (see Beacom et al. 2001). These structures include the Loch Assynt Fault (Fig. 1). The precise age of the 'late-Laxfordian' faulting is poorly constrained, but these structures are unconformably overlain by the unmetamorphosed and little deformed *ca.* 1200 Ma Torridonian Stoer Group. This suggests that the presently exposed parts of the Lewisian Complex had been exhumed to the surface by *ca.* 1200 Ma. Regionally, both the Stoer Group and the Lewisian Complex are unconformably overlain by younger Torridonian sequences (Diabeg and Torridon groups) thought to have been deposited no earlier than 1.1 Ga (Park et al. 1994).

Lewisian host rocks

The Badcallian amphibolite- to granulite-facies TTG gneisses of the Assynt Terrane show foliation development on all scales (e.g., Fig 2a), from millimetres to tens of metres (e.g. Sheraton et al., 1973). The foliation is best developed in intermediate composition gneisses, where it is defined by 0.5 to 5 cm thick layers of contrasting light (plagioclase and quartz) and dark (pyroxene, hornblende and biotite) layers, with individual layers rarely continuing for more than a few metres (Jensen, 1984). Representative samples from the Loch Assynt area typically contain 30% quartz, 20% plagioclase, 10% microcline, 10% orthopyroxene and 30% heavily retrogressed clinopyroxene. Relict grains of the latter mineral are replaced by fine grained intergrown aggregates of chlorite, epidote, actinolite and hornblende.

The Badcallian gneisses were reworked in dextral-reverse shear zones (e.g., the CSZ) during the Inverian, which imposed a NW-SE foliation in the rocks, mainly by reorientation and attenuation of the pre-existing gneissose foliation (e.g., Fig. 2b; Attfield, 1987). Deformation within the Inverian shear zones is extremely heterogeneous, with lenses of lower-strain, more massive material enclosed by anastomosing bands of highly deformed, sheared gneiss (e.g., Attfield, 1987; Chattopadhyay et al., 2010). Representative samples of

reworked Inverian gneisses from within the CSZ contain 20% quartz, 40% feldspar (predominantly plagioclase with alteration bands), 5% pyroxene, 15% hornblende, 15% biotite and chlorite, and 5% other minerals such as epidote. The hornblende, epidote, biotite and chlorite are likely to be a product of the breakdown and hydration of pyroxenes during retrogression (Beach, 1976). The quartz crystals contain 0.25 - 1mm subgrains and form irregular, sub-parallel ribbons of crystals, which are smaller than in the undeformed Badcallian gneisses, possibly due to syn-tectonic recrystallisation (Jensen, 1984).

The Laxfordian event reactivated the central part of the CSZ with a dextral shear sense, producing a new, finer foliation (e.g., Fig. 2d; Sheraton et al., 1973; Attfield, 1978). Commonly, the reworked rocks in both small and large shear zones have a mineralogy that differs significantly from that of the original gneiss and the extent of the changes that occur appears to be in proportion to the intensity of the deformation (e.g., see Beach, 1976). A typical sample of Laxfordian-deformed gneiss from the CSZ contains 75% quartz, 10% hornblende, 10% biotite and muscovite, and 5% feldspar porphyroblasts (typically ~1mm in size). The quartz is banded on a millimetre scale with alternating bands of small quartz grains (<100µm) and larger quartz grains (~500µm to 1mm) which form an anastomosing schistose foliation (Jensen, 1984). Quartz grain boundaries are often pinned by aligned micas and layers richer in mica therefore tend to show finer quartz grain sizes compared to mica-poor layers. The quartz crystals themselves are often elongate and contain poorly developed subgrains. Petrographic observations of Lewisian gneisses show that during regression, pyroxene is first replaced by hornblende which is then replaced by biotite in the most intensely deformed gneisses (Beach, 1976). The Laxfordian reworking occurred in intense zones which anastomose around relict lenses of Badcallian or Inverian gneiss (Sheraton et al., 1973). Tight intrafolial folds are common within the Laxfordian-deformed gneisses and, in places, Inverian folds have been refolded (e.g. on the coast at Port Alltan na Bradhan; see Attfield, 1987; Chattopadhyay et al., 2010). The Scourie dykes within and adjacent to the CSZ have also been pervasively affected by Laxfordian reworking with

shearing particularly concentrated along their margins (Sheraton et al., 1973). Most dykes in the CSZ are sheared into near concordance with the surrounding foliation in the gneisses.

3. Field and Laboratory Methods

3.1. Fieldwork

Fieldwork was carried out visiting well-exposed examples of quartz-pyrite vein localities in the Assynt Terrane and in one area of the Gruinard Terrane (Fig. 1). The relative ages of country rock fabrics and veins were determined at 83 locations using cross-cutting relationships and the orientations of both veins and fabrics were measured. Representative (orientated) hand samples of both country rocks and veins were taken at a number of key localities in order to study deformation microstructures using an optical microscope and also to extract fresh samples of pyrite for Re-Os dating. Having separated appropriate material for dating, we used Re-Os geochronology to determine the age of sulphide (pyrite) mineralization present in several of the quartz veins. We additionally determined sulphur isotope compositions of the dated samples to yield evidence of the origin of the sulphur and by inference the hydrothermal fluids associated with the quartz-pyrite vein formation.

3.2. Rhenium-Osmium Geochronology Analytical Methods

Six pyrite samples co-genetic with quartz veining were analyzed for their rhenium (Re) and osmium (Os) abundances and isotopic compositions. The analyses were conducted at the TOTAL Laboratory for Source Rock Geochronology and Geochemistry at Durham University. The pyrite sample set was collected from five locations: four in the Assynt Terrane and one in the Gruinard Terrane (Fig. 1; Table 1).

The pyrite samples were isolated from the vein host material by crushing, without metal contact, to a < 5 mm grain size. After this stage > 1 g of pyrite was separated from the crushed vein by hand picking under a microscope to obtain a clean mineral separate. The Re and Os analysis reported in this study followed the analytical protocols of Selby et al. (2009). In brief, this involved loading ~ 0.4 g of accurately weighed pyrite into a carius tube

with a known amount of a ^{185}Re and ^{190}Os tracer (spike) solution and 11 ml of inverse *aqua regia* (3 ml 11N HCl and 8 ml 15 N HNO_3). The carius tubes were then sealed and placed in an oven at 220°C for 48 hrs. Osmium was isolated and purified from the acid medium using CHCl_3 solvent extraction and micro-distillation, with Re separated by anion exchange column and single-bead chromatography. The Re and Os fractions were then loaded onto Ni and Pt filaments, respectively, and analyzed for their isotope compositions using negative-ion mass spectrometry on a Thermo Electron TRITON mass spectrometer. Rhenium isotopes were measured statically using Faraday Collectors, with the Os measured in peak hopping mode using the Secondary Electron Multiplier. Total procedural blanks for Re and Os are 2.7 ± 1.1 pg and 0.4 ± 0.4 pg, respectively, with an average $^{187}\text{Os}/^{188}\text{Os}$ of 0.37 ± 0.17 ($n = 2$, 1 SD). The Re and Os uncertainties presented in Table 1 are determined by the full propagation of uncertainties from the mass spectrometer measurements, blank abundances and isotopic compositions, spike calibrations, and the results from analyses of Re and Os standards. The Re standard data together with the accepted $^{185}\text{Re}/^{187}\text{Re}$ ratio (0.59738; Gramlich et al., 1973) are used to correct for mass fractionation. The Re and Os standard solution measurements performed during the two mass spectrometry runs were 0.5982 ± 0.0012 (Re std, $n = 2$) and 0.1608 ± 0.0002 (DROsS, $n = 2$), respectively, which agree with the values reported by Finlay et al. (2011) and references therein.

3.3. Sulphur Isotope Analytical Protocol

Aliquants of pyrite samples for sulphur isotope analysis were taken from the quartz veins at the same five locations as those used for the Re-Os geochronology (Table 1). Approximately 0.01g was used for the analysis, with the sulphur extracted as SO_2 from the pyrite by fusing the sample under vacuum at 1076°C in a Cu_2O (200mg) matrix (Wilkinson & Wyre, 2005). The sample was then analysed on a VG SIRA II mass spectrometer to obtain values for $\delta^{66}\text{SO}_2$ which were converted to $\delta^{34}\text{S}$. Standard correction factors were applied (Craig, 1957). Results are given in conventional $\delta^{34}\text{S}$ notation relative to the Vienna Canon Diablo

troilite standard (V-CDT). The reproducibility based on full replicate analyses of internal laboratory standards was ± 0.2 per mil (1σ).

4. Field relationships of the quartz-pyrite veins

The occurrence of quartz veins is a widely recognised, but little described phenomenon in the rocks of the Assynt Terrane (e.g., the presence of quartz veins is noted in Sheraton et al., 1973). Some generally foliation-parallel veins are clearly relatively late features that are closely associated with shearing along Laxfordian shear zones and the development of schistose, phyllosilicate-rich high strain zones (e.g., Beach, 1976; Beacom, 1999). However, the present study has revealed that an earlier, much more widespread and distinctive group of quartz-pyrite veins are present throughout the Assynt Terrane and at least part of the Gruinard Terrane. The distribution of the quartz veins does not seem uniform – they typically occur in clusters cutting the gneisses in regions covering areas of tens to hundreds of square metres, with particularly well-defined groups recognised in the Loch Assynt and Clashnessie regions of the Assynt Terrane, and along the trace of the CSZ (Fig. 1).

The quartz veins typically range in thickness from a few millimetres to several tens of centimetres (e.g., Fig. 2a-e, g), and are relatively straight and continuous features that can be traced for several metres or, less commonly, tens of metres along strike. They have sharply-defined margins, are occasionally anastomosing and sometimes contain inclusions of country-rock or clusters of pink K-feldspar. Pyrite is not found in all of the veins, but where it occurs it is typically either located along the margins as large crystals (>0.5 mm) or as large clusters (>1 cm) of crystals distributed sparsely throughout the veins (e.g., Fig. 2h). In some cases pyrite clusters have been partially to completely oxidised to hematite or limonite, particularly where they have been exposed at the surface for an extended period; this often gives weathered veins a distinctive localised orange-red staining. Within the CSZ, pyrite crystals are also sometimes found in the sheared gneisses surrounding the vein. In isolated road cut exposures, the development of quartz-pyrite veins is additionally associated with a

localised yellow-brown sulphurous weathering of the gneisses, e.g., in roadcuts east of Lochinver (National grid reference NC 1012 2366; Samples BH2 and 5; Table 1).

4.1. Cross-cutting relationships

The quartz-pyrite veins display a consistent set of cross-cutting relationships with other features in the Lewisian Complex. They typically cross-cut the oldest, moderately to shallowly-dipping Badcallian foliations and folds (e.g., Fig. 2a), although in areas where the foliation is particularly intense and of variable orientation (e.g. Clashnessie), the veins may locally be concordant with the local foliation. The veins also consistently cross-cut the steeply-dipping Inverian shear fabrics of the CSZ (e.g., Fig. 2b) and other minor shear zones of this age within the terrane, as well as all observed Scourie dykes (e.g., Fig. 2c). Both veins and dykes are consistently overprinted and reworked by dextral shear fabrics related to the Laxfordian event, including the development of the central part of the CSZ (Attfield 1987; e.g., Fig. 2d). The quartz veins are also post-dated by 'late Laxfordian', epidote-bearing small-scale shear zones and fractures, which exhibit a predominantly sinistral sense of shear (e.g., Fig. 2e, f; see Beacom et al 2001). Many of the larger quartz vein clasts found in the immediately overlying basal units of the Torridonian sandstones are plausibly derived from the basement veins. The quartz-pyrite veins are everywhere cross-cut by gouge-bearing Phanerozoic (post-Cambrian) normal faults (e.g., NC 1020 2360).

Thus the field observations suggest that the quartz-pyrite veins post-date Badcallian structures, the NW-SE trending Inverian fabrics and Scourie dykes. They appear to pre-date all Laxfordian fabrics, 'late Laxfordian' faults, the deposition of the Torridonian sediments and all post-Torridonian deformation episodes (mainly faulting).

4.2. Orientation and kinematics

The orientations of 140 quartz-pyrite veins measured in the Assynt Terrane during the present study are shown in Figures 3a-c, and the sparse lineations found on the veins in Figure 3aii. A rose diagram plot (Fig. 3ai) suggests a predominance of NE-SW strikes with

subordinate NW-SE trends. The regional stereograms (Figs. 3biv-vi & c) better illustrate the rather wider range of vein orientations, with a reasonably strong concentration of planes striking NE-SW and, to a lesser extent NW-SE. Both sets display bimodal dip directions (e.g., NW or SE and NE or SW, respectively; Figs. 3biv-vi & c). These observations suggest a generally multimodal pattern of fracture orientations.

In order to investigate the possible effects on vein orientation of local country rock fabrics and Laxfordian overprinting, the data have been plotted according to the age of the local fabrics they cross-cut or are reworked by (Fig. 3b). In the regions of gneiss dominated by the Badcallian event, both the foliations (Fig. 3bi) and the veins (Fig. 3biv) have large variations in their orientations. The foliation shows a poorly-defined N-S trend dipping shallowly W, whereas the veins show a reasonably strong NE-SW trend, with bimodal dips steeply to the NW and rather more shallowly to the SE. The Inverian foliation has a strong NW-SE trend with generally steep dips (Fig. 3bii), whereas the veins show a strong NE-SW trend with dips mainly being steep and to the NW (Fig. 3bv). Both the Laxfordian foliation and the veins within the Laxfordian fabrics show a strong NW-SE trend and steep dips (Figs. 3biii and vi), reflecting the strong reworking and reorientation of veins into parallelism with those fabrics during overprinting deformation.

The data have also been plotted according to the localities where well-defined clusters of veins are found (Figs. 3ci-vi). The stereoplots for localities such as Clashnessie and Achmelvich areas (Figs. 3ci-ii) show a wide range of orientations whilst the best defined, statistically significant trend is found in the Loch Assynt cluster (Fig. 3cv). Here there is a very well-defined trend striking NE-SW with the majority of veins dipping steeply NW. It may be significant that the pre-vein Badcallian foliation in this area is much weaker compared to areas such as Clashnessie.

The kinematics of the quartz veins are difficult to deduce with any precision. Most of the veins appear to be dilational (Mode 1 tensile) features based on observed offsets of markers in the adjacent wall rocks, i.e., the vein opening directions lie at high angles to the vein walls). A few large veins in the Loch Assynt and Lochinver regions display regular en

echelon off-shoots (e.g., Fig. 2g) consistent with some degree of vein-parallel shearing during emplacement (e.g. Peacock & Sanderson 1995). Of the seven veins found with such off-shoots, five indicated a sinistral and two a dextral sense of shear. There does not appear to be any obvious orientation control on the shearing directions, suggesting the shearing may be due to local strain heterogeneities. A few veins ($n = 7$) unaffected by Laxfordian reworking display poorly developed mainly oblique mineral lineations on their outer contacts (Fig. 3a_{ii}).

5. Rhenium-Osmium Geochronology

The total Re and Os abundances of the pyrite samples range from 6.8 to 25.8 ppb (parts per billion) and 298.8 to 660.5 ppt (parts per trillion; Table 1), respectively. The majority of the Os within the samples is radiogenic ^{187}Os ($> 92\%$). Four of the samples possess $> 99\%$ radiogenic ^{187}Os (Table 1). As a result, the $^{187}\text{Re}/^{188}\text{Os}$ values are high to very high (265.6 to 17531), with the accompanying $^{187}\text{Os}/^{188}\text{Os}$ values being very radiogenic (11.04 to 675.2). The predominance of radiogenic ^{187}Os ($^{187}\text{Os}'$) in the pyrite samples defines them as Low Level Highly Radiogenic (LLHR; Stein et al., 2000; Morelli et al., 2005). To account for the high-correlated uncertainties between the $^{187}\text{Re}/^{188}\text{Os}$ and $^{187}\text{Os}/^{188}\text{Os}$ data we present the latter with the associated uncertainty correlation value, ρ (Ludwig, 1980), and the 2σ calculated uncertainties for $^{187}\text{Re}/^{188}\text{Os}$ and $^{187}\text{Os}/^{188}\text{Os}$ (Table 1). The regression of all the Re-Os data using *Isoplot V. 3.0* (Ludwig, 2003) and the ^{187}Re decay constant (λ) of $1.666 \times 10^{-11} \text{a}^{-1}$ (Smoliar et al., 1996) yields a Model 3 Re-Os age of 2259 ± 61 (2.9 %) Ma, with an initial $^{187}\text{Os}/^{188}\text{Os}$ of 0.9 ± 9.0 (2σ , Mean Squared Weighted Deviates [MSWD] = 22; Fig. 5a). Although the calculated Re-Os age has only a 2.9 % uncertainty, the high MSWD value (22) suggests that the degree of scatter about the regression line is a function of pyrite Re-Os systematics (discussed below). The imprecision of the initial $^{187}\text{Os}/^{188}\text{Os}$ does not permit an accurate evaluation of the origin of the Os in the pyrite, however the initial $^{187}\text{Os}/^{188}\text{Os}$ value, including the uncertainty, can be used to calculate the abundance of

$^{187}\text{Os}^r$ from the total ^{187}Os (common plus radiogenic) in the pyrite samples ($^{187}\text{Os}^{r1}$; Table 1). The $^{187}\text{Os}^r$ is a product of ^{187}Re decay and model Re-Os dates for each sample can be directly calculated using $t = \ln (^{187}\text{Os}^r / ^{187}\text{Re} = 1) / \lambda$. The model Re-Os dates, with the exception of sample 64.1, all agree - within uncertainty - with the traditional $^{187}\text{Re}/^{188}\text{Os}$ vs $^{187}\text{Os}/^{188}\text{Os}$ isochron age (Table 1; Fig. 5a). One sample from a vein cutting Badcallian gneisses east of Lochinver (64.1; NC 1038, 2249) yields an imprecise model age of 1597 ± 1371.2 Ma. Although this date is within uncertainty of the other model ages and the Re-Os isochron age, its nominal age is significantly younger (~ 800 Ma) than for the other five pyrite samples. As such, sample 64.1 may represent a separate, distinct quartz and pyrite mineralization event. If we consider this to be the case and regress the $^{187}\text{Re}/^{188}\text{Os}$ vs $^{187}\text{Os}/^{188}\text{Os}$ data without sample 64.1, a $^{187}\text{Re}/^{188}\text{Os}$ vs $^{187}\text{Os}/^{188}\text{Os}$ age of 2249 ± 77 Ma, with an initial $^{187}\text{Os}/^{188}\text{Os}$ of 3 ± 13 , is produced (2σ , MSWD = 15; Fig. 5a). This Re-Os isochron age is within uncertainty of that determined from all the Re-Os data, but the degree of scatter about the isochron is reduced (MSWD of 15 vs 22).

Isochron ages can also be determined by the regression of ^{187}Re vs $^{187}\text{Os}^r$ plus their uncertainties. Excluding sample 64.1 for the reasons noted above, the ^{187}Re data together with the $^{187}\text{Os}^r$ values ($^{187}\text{Os}^{r2}$; Table 2) calculated using the initial $^{187}\text{Os}/^{188}\text{Os}$ value (3 ± 13) determined from the $^{187}\text{Re}/^{188}\text{Os}$ vs $^{187}\text{Os}/^{188}\text{Os}$ isochron without sample 64.1 (Fig. 5), a ^{187}Re vs $^{187}\text{Os}^r$ isochron date of 2170 ± 180 Ma is obtained (Fig. 5b, initial $^{187}\text{Os} = 15 \pm 31$ ppt, MSWD = 0.6). We note that with the exception of sample 28 (Lochan Sgeireach) Re-Os model ages calculated using $^{187}\text{Os}^r$ based on the initial $^{187}\text{Os}/^{188}\text{Os}$ value of 3 ± 13 are extremely similar (Table 1). However, sample 28 yields a Model age ~ 450 Ma younger than an age calculated using the initial of 0.9. Both calculated Model ages have very large uncertainties. This sample possesses the least amount of $^{187}\text{Os}^r$ (~ 92 ppt – 73%), with its abundance dramatically affected by the initial $^{187}\text{Os}/^{188}\text{Os}$ value (0.9 vs 3; Table 1).

A weighted average of the model Re-Os ages (not including sample 64.1; calculated using a $^{187}\text{Os}^r$ based on the initial $^{187}\text{Os}/^{188}\text{Os}$ value of 3 ± 13) is 2248 ± 38 (MSWD = 0.6;

Fig. 5c). In summary, the ages determined from both the Re-Os isochron methods and the weighted average of the Re-Os model ages are all within uncertainty. We favour using the $^{187}\text{Re}/^{188}\text{Os}$ vs $^{187}\text{Os}/^{188}\text{Os}$ isochron age (without sample 64-1). From this study we consider the majority of the pyrite mineralization and by inference the precipitation the quartz pyrite veins and fracture formation occurred at 2249 ± 77 Ma.

6. Sulphur Isotope Analysis

All the samples from the sulphur isotope analysis yielded high amounts of sulphur (82 to, 97% yield). The $\delta^{34}\text{S}$ from the sulphides ranges from +3.0 to -2.2 per mil. All the samples are slightly enriched in ^{34}S relative to 0 per mil, with the exception of sample 64.1, which has a slightly depleted value of -2.2. This may suggest a slightly different source of the sulphur for sample 64.1, and coupled with the Re-Os data may support a distinct quartz and pyrite mineralization event from the other five samples. The range in the $\delta^{34}\text{S}$ values (+3.0 and -2.2) encompasses that of the primitive mantle (Rollinson, 1993). The results therefore suggest that the sulphur in the pyrite is most likely derived from a source not isotopically fractionated from the primitive mantle value.

7. Microstructural textures and inferred deformation mechanisms

7.1. Microstructural textures within quartz-pyrite veins

The quartz-pyrite veins display an array of deformation textures suggesting that they have experienced a complex history of deformation at different temperatures and pressures. A number of overprinting relationships are seen which can be related to the relative chronology of events seen in the field. The deformation textures are described below with reference to the age of the country rock fabric which the veins either cross-cut or are overprinted by.

7.1.1 Veins crosscutting Badcallian structures

Despite modest amounts of grain-scale deformation, the veins cross-cutting Badcallian gneisses (e.g., Fig. 2a, e) preserve a diverse range of deformation microstructures. The most deformed examples contain large quartz crystals (> 1mm, but typically 3 – 7mm) that show sweeping undulose extinction and have highly lobate grain boundaries as a result of grain boundary migration processes during recrystallisation (Stipp et al., 2002). Chessboard subgrains (e.g. Fig. 4a) within quartz crystals are also common and form in response to the migration of dislocations within the crystal lattice into subgrain walls during recrystallisation (e.g. Passchier and Trouw, 2005).

The least plastically deformed veins cutting Badcallian foliation are found on the shores of Loch Assynt (e.g., Figs. 2e, g). The quartz crystals within these veins display undulose extinction, whilst some larger grains contain deformation lamellae, which are zones of differently orientated crystal lattice separated by dislocations. Grain boundaries have undergone small-scale bulging during recrystallisation and small grains (<100µm) have developed within the bulges and along the deformation lamellae (e.g., Fig. 4b).

Overall, the range of deformation microstructures observed in the quartz veins cutting Badcallian gneisses suggests that they experienced small amounts of crystal plastic deformation under moderate temperature (400 - 500°C) conditions. The veins on the shore of Loch Assynt locally preserve rather lower temperatures textures (perhaps as low as 300°C) and/or higher strain rate conditions. This may be the result of 'late Laxfordian' deformation associated with slip on the Loch Assynt Fault (e.g., like the structures shown in Figs. 2e, f), to which they are proximal.

7.1.2 Veins cross-cutting Inverian structures

Veins emplaced into Lewisian gneisses reworked by Inverian deformation (e.g., Fig. 2b) also show little obvious deformation at outcrop scale. A range of deformation microstructures are preserved, including undulose extinction, deformation lamellae, new grain growth along crystal boundaries, subgrain development and the development of lobate grain boundaries. These are indicative of recrystallisation under low to moderate temperatures (350 - 500°C)

and high to moderate strain rates. Some veins contain large (>2mm) quartz crystals with lobate boundaries, formed by grain boundary migration under moderate temperatures and strain rates, which show grain boundary bulging and the development of new, small grains (<250µm) within the bulges, particularly at triple-point grain boundaries (Fig. 4c). These structures are typical of recrystallisation under somewhat lower temperatures (300 - 400°C), and may indicate a lower temperature event. There is little evidence for this event within the veins emplaced into Badcallian gneisses, and it may be that it is related to localised later deformation and/or fluid flow restricted to the Inverian shear zones immediately following vein emplacement. Alternatively, it may be a weak manifestation of Laxfordian deformation given the regionally observed coincidence of Inverian and Laxfordian reworking (e.g. Attfield 1987).

7.1.3 Veins overprinted by Laxfordian structures

The veins emplaced within the Laxfordian part of the CSZ (e.g., Fig. 2d) have been heavily reworked at outcrop scale. Many of the grain-scale textures resulting from the recrystallisation of quartz are similar to those seen in the veins which were emplaced into gneisses with Badcallian and Inverian foliations, but the finite strains are much higher. In most veins, larger quartz crystals (>2mm) show sweeping undulose extinction, deformation lamellae, subgrain development and lobate grain boundaries. These microstructures indicate deformation under moderate temperatures (350 - 500°C) and strain rates. Relict S-C' mylonite fabrics (e.g. Berthé et al. 1979; Snoke et al. 1998) are preserved in the most highly deformed veins (e.g., Fig. 4d). Sub-parallel fine-grained (<100 µm) bands of feldspar, muscovite and chlorite define the C-surfaces which are enclosed by polygonal quartz aggregate (with grains sizes 0.5 – 3 mm). Quartz grain boundaries are often pinned by aligned micas and some fine aligned grains are completely enclosed by much larger, undeformed quartz grains (Fig. 4d). These fabrics are typical indicators of significant secondary grain growth under elevated temperature conditions (e.g., Vernon 1976; Passchier and Trouw, 2005).

446

7.1.4 Pyrite microstructural relationships

Pyrite occurs in a variety of forms in the veins of the Assynt Terrane. Some samples contain large clusters of pyrite crystals up to 1.5cm in across (e.g., Fig. 2h) which are intimately intergrown with quartz (e.g., Figs 4e, f). SEM images reveal the partial alteration of pyrite grains to iron oxides along grain margins and fractures within some large pyrite clusters (e.g., Fig. 4g, h). Small (<1mm) pyrite clusters are also associated with the mylonitized quartz veins within the CSZ. There is little evidence for significant deformation of the pyrite grains during recrystallization of the surrounding quartz aggregates even in cases where the intensity of finite plastic strain is high.

456

7.1.5 Summary

The microstructural evidence from the veins suggests that most of the pyrite initially crystallised at the same time as the quartz and that it is therefore a primary mineral phase. The veins then experienced very modest amounts of deformation and recrystallisation during a moderate temperature (350 - 500°C) and low strain rate strain rate event felt throughout most of the Assynt Terrane. Given the similarity in quartz microstructures and interpreted palaeotemperatures with the more highly deformed veins in the CSZ, it seems most likely that the bulk of the modest deformations recorded here are also Laxfordian to 'late Laxfordian' in age (ca. 1780-1400). Laxfordian deformation, especially within the CSZ, resulted in the formation of mylonitic fabrics within the veins under mostly moderate temperatures (350 - 500°C). There may also have been some limited remobilisation and re-precipitation of pyrite related to fluid flow both within the veins and the adjacent sheared gneisses.

470

8. Discussion:

The Re-Os isochron age obtained from the majority of the quartz-pyrite veins (2249 ± 77 Ma) is consistent with our current understanding of the broad ages of regional

474 tectonometamorphic episodes in the Lewisian Complex (Fig. 6). Specifically, they cross cut
 475 older Badcallian (*ca.* 2760 or 2480 Ma) and Inverian (*ca.* 2400-2480 Ma) fabrics and are
 476 overprinted/reworked by younger Laxfordian (1790-1660 Ma) structures. The latter suggests
 477 that the Re-Os systematics were not appreciably disturbed by structural reworking and the
 478 upper greenschist conditions associated with the Laxfordian event.

479 The most recent U-Pb geochronology shows that intrusion of the Scourie dykes
 480 predominantly occurred at 2391 – 2404 Ma, with moderately younger ages (2367 – 2372
 481 Ma) at the SW edge of the Assynt Terrane (Davies and Heaman, 2014). The *ca.* 2250 Ma
 482 age for the quartz-pyrite veins falls within the range of ages obtained from the NW-SE
 483 trending Scourie dyke swarm across the entire Lewisian Complex (Fig. 6; 2418 Ma to 1991
 484 Ma; Chapman 1979; Heaman and Tarney, 1989; Cohen et al., 1988; Waters et al., 1990;
 485 Davies and Heaman, 2014). These studies suggest two main episodes of dyke intrusion at
 486 *ca.* 2418 Ma and 1992 Ma (Fig. 6; Davies and Heaman, 2014), with distinct mantle sources
 487 exploited during each event (Cartwright and Valley, 1991). The idea that there are multiple
 488 episodes of ‘Scourie dyke’ intrusion is consistent with some geological field relationships. It
 489 is known, for example, in the southern region of the Lewisian Complex that some ‘Scourie
 490 dykes’ cut the Loch Maree Group metasediments and metavolcanics, which were thought to
 491 have formed in oceanic basins and accreted to the continental crust through subduction
 492 between 2000 and 1900 Ma (Park et al., 2001).

493 All the quartz-pyrite veins observed during the present study seen in the Assynt
 494 Terrane cross-cut Scourie dykes, although this does not preclude the possibility that
 495 regionally there may be some dykes that are younger. However, the Re-Os pyrite dating of
 496 the veins at *ca.* 2250 Ma suggests a complex polyphase early Palaeoproterozoic tectonic
 497 history of the Lewisian complex (Fig. 6). Veins form by the precipitation of minerals in dilating
 498 hydrofractures and their regional development in clusters and swarms are indicative of
 499 significant phase of fluid flow in the crust (e.g., Sibson, 1996 and references therein). The
 500 simplest types of vein are Mode 1 fractures which open in the direction of the minimum
 501 principle stress and have strike orientations perpendicular to it (e.g., Peacock & Mann,

2005). Most of the veins in the Assynt Terrane appear on the basis of their field relationships to be Mode I features (e.g. Fig. 2a). If so, the prevalence of NE-SW strikes (e.g., Figs. 1, 3ai) implies a NW-SE opening direction, although the veins show a wide range of other orientations (Figs. 3b,c) which are attributed to a number of factors: the presence of highly variable foliation in strongly banded gneisses; the presence of pre-existing fractures, or to the reworking of veins by Laxfordian fabrics.

The pre-Laxfordian NE-SW orientation and inferred NW-SE opening directions of the quartz-pyrite veins lie almost orthogonal to the regional NW-SE orientation – and inferred NE-SW extension direction - of the Scourie dykes. If there are multiple episodes of Scourie dykes on a regional scale, with some pre-dating and some post-dating the quartz-pyrite veins, this implies that there were significant changes in the orientation of regional stress vectors in the 500 Ma period between 2400 and 1900 Ma (Fig. 6). Note, however, that in common with the Scourie dykes, the sulphur isotopic analysis of the quartz-pyrite veins is suggestive of a source not isotopically fractionated from the primitive mantle derivation value (Rollinson, 1993).

Although the Re-Os data for sample 64.1 provide a highly imprecise model age (1597 ± 1356 Ma) its nominal age is considerably younger than the model ages for the other samples (2198.5 – 2328.7 Ma), and, in addition, has the lowest Os abundance of (242.8 ± 33.9 ppb) of all the samples. Furthermore, sample 64.1 is also the only sample with a depleted $\delta^{34}\text{S}$ value (-2.2). Although this value could indicate that the sulphur source is not isotopically fractionated from the primitive mantle value, like the other samples, it may be that the sulphur within the pyrite has a slightly different origin to that found within other veins, or that it may have been disturbed following emplacement, perhaps related to a later phase of 'late Laxfordian' brittle fracture fractures and fluid ingress. Further work and dating is required to verify the age obtained and better constrain the geological and geochronological significance of this younger age.

8.1. Implications for terrane models

Dating of the TTG protoliths suggests that the gneisses of the Gruinard Terrane are at least 100 Ma younger than those of the Assynt Terrane and underwent granulite metamorphism at 2730 Ma (Love et al., 2004; Park, 2005). Thus they are thought to belong to different and separate Archaean terrane which amalgamated along the Strathan Line, south of Lochinver, during Inverian folding and retrogression (Fig. 1, Love et al., 2004). The presence of post-Inverian quartz-pyrite veins within both the Assynt and Gruinard Terranes is consistent with this proposal.

The amphibolite-facies gneisses of the Rhiconich Terrane to the north have yielded protolith ages of 2840-2800 Ma and a record magmatism at 2680 Ma (Kinny and Friend, 1997), but there is no apparent evidence of metamorphism at ca. 2780 Ma. This led Friend and Kinny (2001) to suggest that the Assynt and Rhiconich Terranes were separate Archaean crustal blocks of differing age and early history that were only finally juxtaposed by a major episode of shearing during the along the Laxfordian Shear Zone at ca. 1750 Ma (Fig. 1). This seems consistent with the apparent absence of ca. 2250 Ma quartz-pyrite veins in the Rhiconich Terrane. However, recent fieldwork and dating by Goodenough et al. (2010; 2013) has found evidence that the Laxford Shear Zone initially formed as an Inverian structure, pre-dating the intrusion of a regional suite of arc-related granitic sheets ca. 1880 Ma into both the Assynt and Rhiconich Terranes. These granites are then overprinted by the main Laxfordian deformation and associated amphibolite-facies metamorphism, which ranges from 1790-1670 Ma (Corfu et al., 1994; Kinny and Friend, 1997; Love et al., 2010). In this case the absence of the quartz-pyrite veins to the north of the Laxford Shear Zone is perhaps consistent with significant Laxfordian-age reactivation leading to final juxtaposition of the two terranes.

9. Conclusions

A hitherto unrecognised set of quartz-pyrite veins have been identified in the Assynt and Gruinard terranes of the Lewisian complex. The veins consistently cross-cut Badcallian and Inverian structures in the gneisses, as well as (at least) the majority of Scourie dykes. They

are reworked during Laxfordian shearing events and are also cross cut by a range of later brittle faulting events. The dominant strike direction of the quartz-pyrite veins suggests emplacement during a regional NW-SE extension of the crust, whilst sulphur isotope analyses of the pyrites are consistent with a primitive mantle origin for the fluids.

The Re-Os date of 2249 ± 77 Ma for the pyrite within the veins is consistent with the field relationships and other known geochronological constraints in the Lewisian Complex. Both the Scourie dykes and quartz-pyrite veins are most likely developed as Mode I tensile fractures, but their almost orthogonal present day orientations suggests that whilst the dykes were emplaced during two or more periods of NE-SW crustal extension and associated mafic magmatism ca. 1900-2400 Ma, the quartz-pyrite mineralization ca. 2250 Ma occurred during an intervening phase of NW-SE extension.

The presence of the quartz-pyrite veins in both the Assynt and Gruinard terranes confirms their amalgamation prior to ca. 2250 Ma, most likely during the Inverian. The apparent absence of the veins in the Rhiconich Terrane suggests it may not have been finally amalgamated with the Assynt and Gruinard terranes until the Laxfordian. More generally, this study demonstrates the potential value of the Re-Os technique as a means of dating sulphide mineralisation events in continental basement terrains worldwide.

Acknowledgements

This research was supported, in part, by a student grant from the Geological Society of London to RV. Rob Strachan, an anonymous reviewer and Randy Parrish are thanked for their constructive comments and suggestions as reviewers.

References

- Attfield, P., 1987. The structural history of the Canisp Shear Zone, *In*: Park, R.G. & Tarney, J. (eds), *The early Precambrian rocks of Scotland and related rocks of Greenland*, Department of Geology, Keele, 165-174.
- Beach, A., 1976. The interrelations of fluid transport, deformation, geochemistry and heat flow in early Proterozoic shear zones in the Lewisian complex, *Philosophical Transactions Royal Society London A*, **280**, 569-604.

- Beacom, L.E., 1999. *The Kinematic Evolution of Reactivated and Non-Reactivated Faults in Basement Rocks, NW Scotland*, Unpublished PhD thesis, Queens University, Belfast.
- Beacom, L.E., Holdsworth, R.E., McCaffrey, K.J.W. & Anderson, T.B., 2001. A quantitative study of the influence of pre-existing compositional and fabric heterogeneities upon fracture-zone development during basement reaction, *In*: Holdsworth, R.E., Strachan, R.A., Magloughlin, J.F. & Knipe, R.J, (eds). *The Nature and Tectonic Significance of Fault Zone Weakening*, Geological Society Special Publications, London, **186**, 195-211.
- Berthé, D., Choukroune, P., and Jegouzo, P., 1979. Orthogneiss, mylonite and non coaxial deformation of granites: the example of the South Armorican shear zone. *Journal of Structural Geology*, **1**, 31-43
- Cameron, E.M., 1994. Depletion of gold and LILE in the lower crust: Lewisian Complex, Scotland, *Journal of the Geological Society*, **151**, 747-754.
- Cartwright, I. & Valley, J.W. 1991. Low-¹⁸O Scourie dike magmas from the Lewisian complex, northwestern Scotland. *Geology* **19**, 578-581.
- Chapman, H.J. 1979. 2,390 Myr Rb-Sr whole-rock age for the Scourie dykes of north-west Scotland. *Nature*, **277**, 642-3.
- Chattopadhyay, A., Holdsworth, R.E., McCaffrey, K.J.W. & Wilson, R.W. 2010. Recording and Analyzing Geospatially Accurate Structural Data through 'Digital Mapping' Technique: A Case Study from the Canisp Shear Zone, NW Scotland. *Journal of the Geological Society of India*, **75**, 43-59.
- Cohen, A.S., Waters, F.G., O'Nions, R.K. & O'Hara, M.J., 1988. A precise crystallisation age for the Scourie Dykes, and a new chronology for crustal development in north-west Scotland. *Chemical Geology*, **70**, 19.
- Coleman, M.L. & Moore, M.P., 1978. Direct Reduction of Sulfates to Sulfur Dioxide for Isotopic Analysis, *Analytical Chemical Society*, **50**, 1594-1595.
- Corfu, F., Heaman, L.M. & Rogers, G. 1994: Polymetamorphic evolution of the Lewisian complex, NW Scotland, as recorded by U-Pb isotopic compositions of zircon, titanite and rutile. *Contributions to Mineralogy and Petrology*, **117**, 215-228.
- Coward, M.P. & Park, R.G., 1987. The role of mid-crustal shear zones in the Early Proterozoic evolution of the Lewisian, *In*: Park, R.G. & Tarney, J. (eds), *Evolution of the Lewisian and Comparable Precambrian High Grade Terrains*, Geological Society Special Publications, London, **27**, 127-138.
- Craig, H., 1957. Isotopic standards for carbon and oxygen and correction factors for mass-spectrometric analysis of carbon dioxide, *Geochimica et Cosmochimica*, **12**, 133-149.
- Davies, J.H.F.L. & Heaman, L.M., 2014, New U-Pb baddeleyite and zircon ages for the Scourie dyke swarm: A long-lived large igneous province with implications for the Paleoproterozoic evolution of NW Scotland. *Precambrian Research*, In Press..
- Dickinson, B.B. & Watson, J., 1976. Variations in crustal level and geothermal gradient during the evolution of the Lewisian Complex of Northwest Scotland, *Precambrian Research*, **3**, 363-374.

- Droop, G.T.R., Fernandes, L.A.D. & Shaw, S., 1989. Laxfordian metamorphic conditions of the Palaeoproterozoic Loch Maree Group, Lewisian Complex, NW Scotland, *Scottish Journal of Geology*, **35**, 31-50.
- Finlay, A. J., Selby, D., Osborne, M., 2011. Re-Os geochronology and fingerprinting of United Kingdom Atlantic Margin oil: Temporal Implications for regional petroleum systems, *Geology*, **39**, 475-478.
- Friend, C.R.L. & Kinny, P.D. 1995. New evidence for the protolith ages of Lewisian granulites, northwest Scotland. *Geology*, **23**, 1027–1030.
- Friend, C.R.L. & Kinny, P.D. 2001. A reappraisal of the Lewisian Gneiss Complex: geochronological evidence for its tectonic assembly from disparate terranes in the Proterozoic, *Contribution to Mineralogy and Petrology*, **142**, 198-218.
- Goodenough, K.M., Park, R.G., Krabbendam, M., Myers, J.S., Wheeler, J., Loughlin, S., Crowley, Q., L.F.C.R., Beach, A., Kinny, P.D., Graham, R., 2010. The Laxford Shear Zone: an end-Archaean terrane boundary? In: Law, R., Butler, R.W.H., Holdsworth, R.E., Krabbendam, M., Strachan, R. (eds.), *Continental Tectonics and Mountain Building*. Geological Society Special Publication, **335**, 103-120.
- Goodenough, K.M., Crowley, Q.G., Krabbendam, M. & Parry, S.E. 2013. New U-Pb age constraints for the Laxford Shear Zone, NW Scotland: Evidence for tectono-magmatic processes associated with the formation of a Palaeoproterozoic supercontinent. *Precambrian Research*, **233**, 1-19.
- Gramlich, J.W., Murphy, T.J., Garner, E.L. & Shields, W.R., 1973. Absolute isotopic abundance ratio and atomic weight of a reference sample of rhenium, *Journal of Research of the National Bureau of Standards*, **77A**, 691–698.
- Hamilton, P.J., Evensen, N.M., O’Nions, R.K., Tarney, J., 1979. Sm-Nd systematics of Lewisian gneisses: implications for the origin of granulites. *Nature*, **277**, 25–28.
- Heaman, L.M. & Tarney, J., 1989. U-Pb baddeleyite ages for the Scourie dyke swarm, Scotland: evidence for two distinct intrusion events, *Nature*, **340**, 705-708.
- Jensen, L.N., 1984. Quartz microfabric of the Laxfordian Canisp Shear Zone, NW Scotland, *Journal of Structural Geology*, **6**, 293-302.
- Kinny, P., Friend, C., 1997. U-Pb isotopic evidence for the accretion of different crustal blocks to form the Lewisian Complex of Northwest Scotland. *Contributions to Mineralogy and Petrology*, **129**, 326–340.
- Kinny, P.D., Friend, C.R.L. & Love, G.L., 2005. Proposal for a terrane-based nomenclature for the Lewisian Gneiss Complex of NW Scotland, *Journal of the Geological Society*, **162**, 175-186.
- Love, G.J.L, Kinny, P.D. & Friend, C.R.L., 2004. Timing of magmatism and metamorphism in the Gruinard Bay area of the Lewisian Gneiss Complex: comparisons with the Assynt Terrane and implications for terrane accretion, *Contributions to Mineralogy and Petrology*, **146**, 620-636.
- Love, G.J., Friend, C.R.L., Kinny, P.D., 2010. Palaeoproterozoic terrane assembly in the Lewisian Gneiss Complex on the Scottish mainland, south of Gruinard Bay: SHRIMP U–Pb zircon evidence. *Precambrian Research*, **183**, 89–111.

- Ludwig, K.R., 1980, Calculation of uncertainties of U-Pb isotope data: *Earth and Planetary Science Letters*, **46**, 212–220.
- Ludwig, K.R., 2003, Isoplot/Ex, version 3: A geochronological toolkit for Microsoft Excel: Berkeley, CA, Geochronology Center Berkeley.
- Moorbath, S., Welke, H., Gale, N., 1969. The significance of lead isotope studies in ancient, high-grade metamorphic basement complexes, as exemplified by the Lewisian rocks of Northwest Scotland. *Earth and Planetary Science Letters*, **6**, 245–256.
- Morelli, R.M., Creaser, R.A., Selby, D., Kontak, D.J. and Horne, R.J., 2005, Rhenium-Osmium arsenopyrite geochronology of Meguma Group gold deposits, Meguma terrane, Nova Scotia, Canada: Evidence for multiple gold mineralizing events, *Economic Geology*, **100**, 1229–1242.
- O'Hara, M.J. 1961. Petrology of the Scourie Dyke, Sutherland. *Mineralogical Magazine*, **32**, 848-865.
- Park, R.G., 1970. Observations on Lewisian chronology. *Scottish Journal of Geology*, **6**, 379–399.
- Park, R.G., 2005. The Lewisian terrane model: a review, *Scottish Journal of Geology*, **41**, 105-118.
- Park., R.G. & Tarney, J., 1987. The Lewisian Complex: a typical Precambrian high-grade terrane?, In: Park, R.G. & Tarney, J. (eds), *Evolution of the Lewisian and Comparable Precambrian High Grade Terranes*, Geological Society, London, 13-26.
- Park, R.G., Cliff, R.A., Fettes, D.J., Stewart A.D., 1994. Precambrian rocks in northwest Scotland west of the Moine Thrust: the Lewisian Complex and the Totridonian. In: W. Gibbons and A.L. Harris (Editors), *A Revised Correlation of Precambrian Rocks in the British Isles*. Geological Society of London Special Report, **22**, 6-22.
- Park, R.G, Tarney, J. & Connelly, J.N., 2001. The Loch Maree Group: Palaeoproterozoic subduction-accretion complex in the Lewisian of NW Scotland, *Precambrian Research*, **105**, 205-226.
- Park, R.G., Stewart, A.D. & Wright, D.T. 2002. The Hebridean Terrane. In: Trewin, N.H. (ed) *The Geology of Scotland*. Geological Society, London, 45-80.
- Passchier, C.W. & Trouw, R.A.J., 2005. *Micro-Tectonics*, Springer Berlin Heidelberg, New York, 25-66.
- Peacock, D.C.P. & Mann, A., 2005. Evaluation of the controls on fracturing in reservoir rocks, *Journal of Petroleum Geology*, **28**, 385-396.
- Peacock, D.C.P. & Sanderson, D.J. 1995. Pull-aparts, shear fractures and pressure solution. *Tectonophysics*, 241, (1-2), 1-13.
- Rollinson, H., 1993. *Using Geochemical Data: evaluation, presentation, interpretation*, Longman Group UK Ltd, Harlow, 303-306.

- Selby, D., Kelley, K.D., Hitzman, M.W. & Zieg, J., 2009. Re-Os sulphide (Bornite, Chalcopyrite, and Pyrite) systematic of the Carbonate-hosted copper deposits at Ruby Creek, Southern Brooks Range, Alaska, *Economic Geology*, **104**, 437-444.
- Sibson, R.H. 1996. Structural permeability of fluid-driven fault-fracture meshes. *Journal of Structural Geology*, **18**, 1031–1042.
- Sheraton, J.W., Tarney, J., Wheatley, T.J. & Wright, A.E., 1973. The structural history of the Assynt district, In: Park, R.G. & Tarney, J. (eds), *The early Precambrian rocks of Scotland and related rocks of Greenland*, Department of Geology, Keele, 13-30.
- Smoliar, M.I., Walker, R.J., & Morgan, J.W., 1996. Re-Os isotope constraints on the age of Group IIA, IIIA, IVA, and IVB iron meteorites, *Science*, **271**, 1099–1102.
- Snoke, A.W., Tullis, J. and Todd, V.R., 1998. *Fault-related Rocks*. Princeton University Press, Princeton New Jersey, New Jersey, 617 pp.
- Stein, H.J., Morgan, J.W. & Schersten, A., 2000. Re-Os of Low-Level Highly Radiogenic (LLHR) Sulphides: The Hurnas Gold Deposit, Southwest Sweden, Records Continental-Scale Tectonic Events, *Economic Geology*, **95**, 1657-1671.
- Stipp, M., Stunitz, H., Heilbronner, R. & Schmid, S.M., 2002. The eastern Tonale fault zone: a 'natural laboratory' for crystal plastic deformation of quartz over a temperature range from 250 to 700°C, *Journal of Structural Geology*, **24**, 1861-1884.
- Sutton, J. & Watson, J., 1951. The pre-Torridonian metamorphic history of the Loch Torridon and Scourie areas in the north-west Highlands, and its bearing on the chronological classification of the Lewisian, *Quarterly Journal of the Geological Society*, **106**, 241-307.
- Tarney, J., 1973. The Scourie dyke suite and the nature of the Inverian event in Assynt, In: Park, R.G. & Tarney, J. (eds), *The early Precambrian rocks of Scotland and related rocks of Greenland*, Department of Geology, Keele, 31-44.
- Vernon, R.H. 1976. *Metamorphic Processes: Reactions and Microstructure Development*. George Allen & Unwin, pp 247.
- Waters, F.G., Cohen, A.S., O'Nions, R.K. & O'Hara, M.J., 1990. Development of Archaean lithosphere deduced from chronology and isotope chemistry of Scourie Dykes, *Earth and Planetary Science Letters*, **97**, 241-255.
- Wheeler, J., Park, R.G., Rollinson, H.R. & Beach, A., 2010. The Lewisian Complex: insights into deep crustal evolution, In: Law, R.D., Butler, R.W., Holdsworth, R.E., Krabbendam, M. & Strachan, R.A. (eds), *Continental Tectonics and Mountain Buildings: The Legacy of Peach and Horne*, Geological Society, London, Special Publications, **335**, 51-79.
- Wilkinson, J.J. & Wyre, S.L., 2005. Ore-Forming Processes in Irish-Type Carbonate-hosted Zn-Pb Deposits: Evidence from Mineralogy, Chemistry, and Isotopic Composition of Sulphides at the Lisheen Mine. *Economic Geology*, **100**, 63-86.
- Zhu, X.K., O'Nions, R.K., Belshaw, N.S., Gibb, A.J., 1997. Lewisian crustal history from in situ SIMS mineral chronometry and related metamorphic textures. *Chemical Geology*, **136**, 205–218.

Figure Captions

Figure 1) Highly simplified geological map showing the location and orientations of the quartz vein clusters (i-vi) studied within the Assynt Terrane of the Lewisian Complex. Note that this is not an exhaustive assessment of all quartz veins present in the Assynt Terrane, i.e. there may be many more clusters than are shown here. Inset map shows general location in Scotland and main Lewisian Complex terranes discussed in this paper.

Figure 2) Field relationships of quartz-pyrite veins. a) NE-SW vein cross-cutting shallowly-NW-dipping Badcallian foliation near Clashnessie (NC 0855 3102). Note offset of layers across vein indicating Mode I tensile opening (arrows); b) NE-SW vein (below hammer) cross-cutting steep NW-SE Inverian foliation in Canisp Shear Zone (NC 0521 2593); c) NE-SW vein cross-cutting Scourie dyke on the shore of Loch Assynt (NC 2135 2510); d) NW-SE vein folded and reworked by Laxfordian fabrics, Canisp Shear Zone (NC 0515 2620); e) NE-SW vein cut and offset 10cm by NW-SE sinistral brittle fault in Badcallian gneisses close to the trace of the Loch Assynt Fault (NC 2110 2517); f) En echelon tensile fractures filled with epidote indicating sinistral shear in Badcallian gneisses close to the trace of the Loch Assynt Fault (NC 2110 2517); g) ENE-WSW vein with en-echelon off-shoots, indicating a small component of sinistral shear parallel to the vein margins (NC 2135 2510); h) Large pyrite cluster within a quartz vein (NC1038 2249). Note fracturing of pyrite and characteristic iron oxide staining.

Figure 3) Orientation data for the regional quartz-pyrite vein suite. a) i) Rose diagram of vein trends for the entire Assynt Terrane (for locality-based versions, see Fig. 1), ii) lower hemisphere equal-area stereoplot of veins with lineated margins; b) Equal area stereoplots of gneiss foliations (i-iii) and of associated veins from each locality (iv-vi) grouped according to the inferred age of the wall rock fabric; c) Equal area stereoplots of quartz vein clusters measured in the six localities (i-vi) shown in Fig 1.

Figure 4) Representative microstructures of quartz-pyrite veins viewed using optical microscope and FESEM. a) Chess-board extinction in large quartz crystals from vein cutting

Badcallian gneisses at Kylesku; b) New grains forming along grain boundaries and deformation lamellae, reflecting slightly lower temperature overprint in vein located close to the trace of the Loch Assynt Fault; c) Development of new grains at triple junction grain boundaries overprinting higher temperature deformation features in vein cutting Inverian fabrics near Lochinver; d) Recrystallised S-C fabric in highly sheared veing from the Laxfordian central part of the Canisp Shear Zone, e) Quartz intergrown with within blocky pyrite cluster; f) Intricate intergrowths of pyrite and quartz from vein cutting Scourie dyke at Loch Assynt; g) BSEM image of smooth pyrite (light grey) intergrown with quartz (dark grey) from the same sample as f). The radial fibrous material is iron oxide replacing pyrite; h) Alteration of pyrite (bright grey) along fractures to iron oxides (darker mottled greys), Sample 64.1 (see text for details). Note that all the optical micrographs are cross-polar views.

Figure 5) Re-Os data for the pyrite from the quartz-pyrite veins. A) $^{187}\text{Re}/^{188}\text{Os}$ and $^{187}\text{Os}/^{188}\text{Os}$ plot for all samples and all samples minus sample 64.1; B) ^{187}Re vs $^{187}\text{Os}^r$ plot, with the $^{187}\text{Os}^r$ data calculated using an initial of 3 ± 13 ; C) Weighted average of Re-Os model ages, with the model ages calculated using an initial of 3 ± 13 . See text for discussion.

Figure 6) The chronology of events during the Archaean to Proterozoic in the Assynt Terrane, showing the range of possible Scourie dyke episodes and the vein emplacement period ascertained during the present study.

Table Caption

Table 1) Re-Os and S isotope data for pyrite from quartz veins in the Lewisian Complex, NW Scotland. All uncertainities are reported at the 2s level, $^{187}\text{Os}/^{188}\text{Os}$ uncertainities reported at 2SE; all data are blank corrected, blanks for Re and Os were 2.7 ± 1.1 and 0.40 ± 0.42 pg, respectively, with an average $^{187}\text{Os}/^{188}\text{Os}$ value of 0.37 ± 0.17 (1SD, $n = 2$). All uncertainities

are determined through the full propagation of uncertainties of the Re and Os mass spectrometer measurements, blank abundances and isotopic compositions, spike calibrations, and reproducibility of standard Re and Os isotopic values. $^{187}\text{Os}^r$ presented are calculated using initial $^{187}\text{Os}/^{188}\text{Os}$, plus its uncertainty, from regression of data using $^{187}\text{Re}/^{188}\text{Os}$ vs. $^{187}\text{Os}/^{188}\text{Os}$ isochron plot; rho is the error correlation.

1= $^{187}\text{Os}^r$ determined from an initial $^{187}\text{Os}/^{188}\text{Os}$ of 0.9 ± 9.0 (Fig. 5A).

2= $^{187}\text{Os}^r$ determined from an initial $^{187}\text{Os}/^{188}\text{Os}$ of 3 ± 13 (Fig. 5A). With the exception of sample RO297-3/28, the calculated % $^{187}\text{Os}^r$ is very similar using either initial $^{187}\text{Os}/^{188}\text{Os}$ values of 0.9 ± 9.0 or 3 ± 13 . For sample RO297-3/28 the % $^{187}\text{Os}^r$ decreases to ~72.8% using an initial $^{187}\text{Os}/^{188}\text{Os}$ value of 3 ± 13 . A model age can be directly calculated using

$$^{187}\text{Os}^r/^{187}\text{Re} = e^{t\lambda} - 1$$

3 = Model age determined using an initial $^{187}\text{Os}/^{188}\text{Os}$ value of 0.9 ± 9.0 (Fig. 5A).

4 = Model age determined using an initial $^{187}\text{Os}/^{188}\text{Os}$ value of 3 ± 13 (Fig. 5A).

5 = The reproducibility based on full replicate analyses of internal laboratory standards was ± 0.2 per mil (1σ).

876

1
2
3 1
4 2 Structural characteristics and Re-Os dating of quartz-pyrite veins in the
5
6
7 3 Lewisian Gneiss Complex, NW Scotland: evidence of an Early
8
9 4 Paleoproterozoic hydrothermal regime during terrane amalgamation.
10
11 5

12
13 6 R. Vernon^{1*}, R.E. Holdsworth^{1†}, D. Selby¹, E. Dempsey¹, A. ~~J.~~ Finlay¹ & ~~A.F.~~ E. Fallick²
14
15 7

16
17 8 ¹ Department of Earth Sciences, Durham University, Durham, DH1 3LE, UK.

18
19 9 ² SUERC, Scottish Enterprise Technology Park, Rankine Avenue, East Kilbride, G75 0QF,
20
21 10 UK.

22 11 *Current address: Department of Geology, University of Leicester, University Road,
23
24 12 Leicester, LE1 7RH, UK.

25
26 13 [†]Corresponding author
27
28 14

29
30 15 **Abstract:** In the Archaean basement rocks of the Assynt and Gruinard terranes of the
31
32 16 mainland Lewisian Complex in NW Scotland, a regional suite of quartz-pyrite veins cross-cut
33
34 17 regional Palaeoproterozoic (Badcallian, ~~ca.~~ 2700 Ma; Inverian, ~~ca.~~ 2480 Ma) fabrics
35
36 18 and associated Scourie dykes. The quartz veins are overprinted by amphibolite-greenschist
37
38 19 facies Laxfordian deformation fabrics (~~ca.~~ 1760 Ma) and later brittle faults. The
39
40 20 hydrothermal mineral veins comprise a multimodal system of tensile/hybrid hydraulic
41
42 21 fractures which are inferred to have formed during a regional phase of NW-SE extension.
43
44 22 The almost orthogonal orientation of the quartz veins (NE-SW) to the Scourie dykes (NW-
45
46 23 SE) are incompatible and must result from distinct paleostress regimes suggesting they are
47
48 24 related to different tectonic events. This hypothesis is supported by Rhenium-Osmium dating
49
50 25 of pyrite that yields an age of 2249 ± 77 Ma, placing the vein-hosted mineralisation event
51
52 26 after the oldest published dates for the Scourie Dykes (2420 Ma), but before the youngest
53
54 27 ages (1990 Ma). Sulphur isotope analysis suggests that the sulphur associated with the
55
56
57
58
59
60
61
62
63
64
65

pyrite is isotopically indistinguishable from~~ef~~ primitive mantle~~-origin~~. The presence of the
2250 Ma quartz-pyrite veins in both the Assynt and Gruinard terranes confirms that
these crustal units were amalgamated during or prior to Inverian deformation. The absence
of the veins in the Rhiconich Terrane is consistent with the suggestion that it was not finally
amalgamated to the Assynt Terrane until the Laxfordian.

[End]

1. Introduction

The Archaean gneisses of the Lewisian Complex in NW Scotland form a well exposed and relatively accessible area of Laurentian continental basement rocks that lie in the immediate foreland region of the Palaeozoic Caledonian Orogen (Fig. 1). Like many regions of continental metamorphic basement, the Lewisian Complex preserves evidence for multiple episodes of igneous intrusion, ductile and brittle deformation together with associated phases of metamorphism and mineralisation (e.g. Sutton and Watson 1951; Park 1970; Beacom et al., 2001; Wheeler et al., 2010). Whilst cross-cutting and overprinting relationships observed in the field and thin section allow *relative* age relationships to be established on both regional and local scales, only radiometric ages are able to give information concerning the absolute timing of events. Despite the emergence of an increasing number of geochronometers for Earth Scientists, an enduring problem in many basement regions is a relative paucity of material suitable for reliable radiometric dating. This lack of absolute age determinations has become a particularly significant problem in the Lewisian Complex since Kinny et al. (2005) and Friend and Kinny (2001) proposed that the Lewisian may comprise a number of lithologically and geochronologically distinct tectonic units or terranes assembled progressively during a series of Precambrian amalgamation episodes perhaps spanning more than a billion years (see Park, 2005; Goodenough et al., 2013 for discussions).

This paper describes the lithology, field relationships and microstructures of a little described set of quartz-pyrite veins that are recognised throughout the Assynt Terrane and within the Gruinard Terrane. These mineralised hydrofractures display a consistent set of contact relationships relative to regionally recognised igneous, metamorphic and deformational events. Rhenium-osmium (Re-Os) geochronology on pyrites collected from these veins is used to obtain a consistent set of ages that better constrain the absolute timing of events in this important part of the Lewisian Complex in NW Scotland. It also illustrates the potential value of the Re-Os technique as a means of dating sulphide mineralisation events in geologically complex continental basement terrains worldwide.

2. Regional Setting

The Precambrian rocks of the Lewisian Complex of NW Scotland form a fragment of the continental basement of Laurentia that lies to the west of the Caledonian Moine Thrust (Fig. 1). The rocks are for the most part little affected by Caledonian deformation and have experienced a number of major crustal-scale geological events during the Archaean and Palaeoproterozoic. The Lewisian Complex is divided into a number of tectonic regions or terranes which are predominantly separated by steeply-dipping shear zones or faults (e.g. Park et al., 2002; Park, 2005).

The Assynt Terrane (Fig. 1) forms the central part of the Lewisian Complex in mainland NW Scotland. It comprises grey, banded, tonalite-trondjemite-granodioritic (TTG) gneisses which are locally highly heterogeneous lithologically, ranging from ultramafic to acidic compositions (e.g., Sheraton et al., 1973). The TTG gneisses are thought to be derived from igneous plutons intruded at 3030 to 2960 Ma (high precision U-Pb and Sm-Nd geochronology; Hamilton et al., 1979; Friend and Kinny, 1995; Kinny and Friend, 1997). These rocks then underwent deformation and granulite-facies metamorphism during the so-called Badcallian event(s) which led to significant depletion of large-ion lithophile elements in the TTG gneisses that is more extensive in the Assynt Terrane compared to adjacent amphibolite-facies terranes (e.g. Rhiconich, Gruinard; Moorbath et al., 1969; Cameron, 1994; Wheeler et al., 2010). The timing of Badcallian events are incompletely resolved with current age constraints suggesting either ~~ca.~~ 2760 Ma (e.g., Corfu et al. 1994; Zhu et al., 1997), and/or ~~ca.~~ 2490 - 2480 Ma (e.g., Friend and Kinny 1995; Kinny & Friend, 1997).

The central part of the Assynt Terrane is cut by the major NW-SE-trending, steeply dipping dextral transpressional Canisp Shear Zone (CSZ) which has a maximum width of 1.5km (Attfield, 1987; Fig. 12). There are also many other smaller steeply-dipping, NW-SE to WNW-ESE trending minor shear zones cutting the surrounding Badcallian gneisses (Park and Tarney, 1987). Some of these shear zones, including the CSZ, developed initially during Inverian deformation and amphibolites-facies retrogression which affected substantial parts

of the Assynt Terrane. The absolute age of this event is the subject of significant uncertainty and debate, with a majority of studies considering it to be ~~eaca.~~ 2490 - 2480 Ma (e.g., Corfu et al. 1994; Love et al., 2004; Goodenough et al., 2013). Others (e.g., Friend and Kinny 1995; Kinny and Friend, 1997) suggest that the Inverian is a younger – as yet undated – event younger than ~~eaca.~~ 2480 Ma while still pre-dating the oldest Scourie dykes. These mafic to ultramafic Scourie dykes are found throughout the Assynt Terrane, ranging in thickness from a few mm to several tens of m and were intruded ~~eaca.~~ 1900 - 2400 Ma (Rb-Sr whole rock and U-Pb geochronology; Chapman 1979; Heaman & Tarney, 1989; Davies & Heaman 2014³). The NW-SE-trending Scourie dykes cross-cut local Inverian fabrics and display evidence of having been emplaced under amphibolite facies pressures and temperatures, i.e. in the middle crust, possibly immediately following the Inverian event (O'Hara, 1961; Tarney, 1973; Wheeler et al., 2010).

In the Assynt Terrane, the significantly later main phase Laxfordian event has traditionally been associated with the shearing of the Scourie dykes and widespread retrogression of the TTG gneisses under lower amphibolite to upper greenschist-facies metamorphic conditions (e.g., Sutton and Watson, 1951; Attfield, 1987; Beacom et al., 2001). The Laxfordian is recognised throughout much of the Lewisian complex and appears to be a long lived series of events starting with a series of magmatic events ~~eaca.~~ 1900-1870 Ma – at least some of which are related to island arc development – followed by a protracted orogenic episode lasting from 1790 - 1660 Ma (see discussion in Goodenough et al., 2013). The effects of Laxfordian reworking in the Assynt Terrane are highly localised, being largely restricted to the central part (~~eaca.~~ 1km wide) of the CSZ and other shear zones, as well as along the margins of the Scourie dykes. This contrasts with the neighbouring Rhiconich and Gruinard Terranes where the Laxfordian event reached amphibolite facies and was associated with more pervasive ductile shearing and reworking (Droop et al., 1989). This has led to the suggestion that the Assynt Terrane represents a shallower depth crustal block during the Laxfordian (e.g., Dickinson and Watson, 1976; Coward and Park, 1987).

In the Assynt and Guinard terranes, a younger set of 'late Laxfordian' sinistral low greenschist-facies mylonitic shear zones, brittle faults and localized folds is recognised developed sub-parallel to the pre-existing high-strain fabrics in Laxfordian and Inverian shear zones (see Beacom et al. 2001). These structures include the Loch Assynt Fault (Fig. 1). The precise age of the 'late-Laxfordian' faulting is poorly constrained, but these structures are unconformably overlain by the unmetamorphosed and little deformed ca. 1200 Ma Torridonian Stoer Group. This suggests that the presently exposed parts of the Lewisian Complex had been exhumed to the surface by ca. 1200 Ma. Regionally, both the Stoer Group and the Lewisian Complex are unconformably overlain by younger Torridonian sequences (Diabeg and Torridon groups) thought to have been deposited no earlier than 1.1 Ga (Park et al. 1994).

Lewisian host rocks

The Badcallian amphibolite- to granulite-facies TTG gneisses of the Assynt Terrane show foliation development on all scales (e.g., Fig 2a), from millimetres to tens of metres (e.g. Sheraton et al., 1973). The foliation is best developed in intermediate composition gneisses, where it is defined by 0.5 to 5 cm thick layers of contrasting light (plagioclase and quartz) and dark (pyroxene, hornblende and biotite) layers, with individual layers rarely continuing for more than a few metres (Jensen, 1984). Representative samples from the Loch Assynt area typically contain 30% quartz, 20% plagioclase, 10% microcline, 10% orthopyroxene and 30% heavily retrogressed clinopyroxene. Relict grains of the latter mineral are replaced by fine grained intergrown aggregates of chlorite, epidote, actinolite and hornblende.

The Badcallian gneisses were reworked in dextral-reverse shear zones (e.g., the CSZ) during the Inverian, which imposed a NW-SE foliation in the rocks, mainly by reorientation and attenuation of the pre-existing gneissose foliation (e.g., Fig. 2b; Attfield, 1987). Deformation within the Inverian shear zones is extremely heterogeneous, with lenses of lower-strain, more massive material enclosed by anastomosing bands of highly deformed, sheared gneiss (e.g., Attfield, 1987; Chattopadhyay et al., 2010). Representative

samples of reworked Inverian gneisses from within the CSZ contain 20% quartz, 40% feldspar (predominantly plagioclase with alteration bands), 5% pyroxene, 15% hornblende, 15% biotite and chlorite, and 5% other minerals such as epidote. The hornblende, epidote, biotite and chlorite are likely to be a product of the breakdown and hydration of pyroxenes during retrogression (Beach, 1976). The quartz crystals contain 0.25 - 1mm subgrains and form irregular, sub-parallel ribbons of crystals, which are smaller than in the undeformed Badcallian gneisses, possibly due to syn-tectonic recrystallisation (Jensen, 1984).

The Laxfordian event reactivated the central part of the CSZ with a dextral shear sense, producing a new, finer foliation (e.g., Fig. 2d; Sheraton et al., 1973; Attfield, 1978). Commonly, the reworked rocks in both small and large shear zones have a mineralogy that differs significantly from that of the original gneiss and the extent of the changes that occur appears to be in proportion to the intensity of the deformation (e.g., see Beach, 1976). A typical sample of Laxfordian-deformed gneiss from the CSZ contains 75% quartz, 10% hornblende, 10% biotite and muscovite, and 5% feldspar porphyroblasts (typically ~1mm in size). The quartz is banded on a millimetre scale with alternating bands of small quartz grains (<100µm) and larger quartz grains (~500µm to 1mm) which form an anastomosing schistose foliation (Jensen, 1984). Quartz grain boundaries are often pinned by aligned micas and layers richer in mica therefore tend to show finer quartz grain sizes compared to mica-poor layers. The quartz crystals themselves are often elongate and contain poorly developed subgrains. Petrographic observations of Lewisian gneisses show that during regression, pyroxene is first replaced by hornblende which is then replaced by biotite in the most intensely deformed gneisses (Beach, 1976). The Laxfordian reworking occurred in intense zones which anastomose around relict lenses of Badcallian or Inverian gneiss (Sheraton et al., 1973). Tight intrafolial folds are common within the Laxfordian-deformed gneisses and, in places, Inverian folds have been refolded (e.g. on the coast at Port Alltan na Bradhan; see Attfield, 1987; Chattopadhyay et al., 2010). The Scourie dykes within and adjacent to the CSZ have also been pervasively affected by Laxfordian reworking with

shearing particularly concentrated along their margins (Sheraton et al., 1973). Most dykes in the CSZ are sheared into near concordance with the surrounding foliation in the gneisses.

3. Field and Laboratory Methods

3.1. Fieldwork

Fieldwork was carried out visiting well-exposed examples of quartz-pyrite vein localities in the Assynt Terrane and in one area of the Gruinard Terrane (Fig. 1). The relative ages of country rock fabrics and veins were determined at 83 locations using cross-cutting relationships and the orientations of both veins and fabrics were measured. Representative (orientated) hand samples of both country rocks and veins were taken at a number of key localities in order to study deformation microstructures using an optical microscope and also to extract fresh samples of pyrite for Re-Os dating. Having separated appropriate material for dating, we used Re-Os geochronology to determine the age of sulphide (pyrite) mineralization present in several of the quartz veins. We additionally determined sulphur isotope compositions of the dated samples to yield evidence of the origin of the sulphur and by inference the hydrothermal fluids associated with the quartz-pyrite vein formation.

3.2. Rhenium-Osmium Geochronology Analytical Methods

Six pyrite samples co-genetic with quartz veining were analyzed for their rhenium (Re) and osmium (Os) abundances and isotopic compositions. The analyses were conducted at the TOTAL Laboratory for Source Rock Geochronology and Geochemistry at Durham University. The pyrite sample set was collected from five locations: four in the Assynt Terrane and one in the Gruinard Terrane (Fig. 1; Table 1).

The pyrite samples were isolated from the vein host material by crushing, without metal contact, to a < 5 mm grain size. After this stage > 1 g of pyrite was separated from the crushed vein by hand picking under a microscope to obtain a clean mineral separate. The Re and Os analysis reported in this study followed the analytical protocols of Selby et al. (2009). In brief, this involved loading ~ 0.4 g of accurately weighed pyrite into a carius tube

with a known amount of a ^{185}Re and ^{190}Os tracer (spike) solution and 11 ml of inverse *aqua regia* (3 ml 11N HCl and 8 ml 15 N HNO_3). The carius tubes were then sealed and placed in an oven at 220°C for 48 hrs. Osmium was isolated and purified from the acid medium using CHCl_3 solvent extraction and micro-distillation, with Re separated by anion exchange column and single-bead chromatography. The Re and Os fractions were then loaded onto Ni and Pt filaments, respectively, and analyzed for their isotope compositions using negative-ion mass spectrometry on a Thermo Electron TRITON mass spectrometer. Rhenium isotopes were measured statically using Faraday Collectors, with the Os measured in peak hopping mode using the Secondary Electron Multiplier. Total procedural blanks for Re and Os are 2.7 ± 1.1 pg and 0.4 ± 0.4 pg, respectively, with an average $^{187}\text{Os}/^{188}\text{Os}$ of 0.37 ± 0.17 ($n = 2$, 1 SD). The Re and Os uncertainties presented in Table 1 are determined by the full propagation of uncertainties from the mass spectrometer measurements, blank abundances and isotopic compositions, spike calibrations, and the results from analyses of Re and Os standards. The Re standard data together with the accepted $^{185}\text{Re}/^{187}\text{Re}$ ratio (0.59738; Gramlich et al., 1973) are used to correct for mass fractionation. The Re and Os standard solution measurements performed during the two mass spectrometry runs were 0.5982 ± 0.0012 (Re std, $n = 2$) and 0.1608 ± 0.0002 (DROsS, $n = 2$), respectively, which agree with the values reported by Finlay et al. (2011) and references therein.

3.3. Sulphur Isotope Analytical Protocol

Aliquants of pyrite samples for sulphur isotope analysis were taken from the quartz veins at the same five locations as those used for the Re-Os geochronology (Table 1). Approximately 0.01g was used for the analysis, with the sulphur extracted as SO_2 from the pyrite by fusing the sample under vacuum at 1076°C in a Cu_2O (200mg) matrix (Wilkinson & Wyre et al., 2005). ~~The method of Coleman & Moore (1973) was followed for extracting sulphur from SO_2 from sulphates and. The sample was then~~ analysed on a VG SIRA II mass spectrometer to obtain values for $\delta^{66}\text{SO}_2$ which were converted to $\delta^{34}\text{S}$. Standard correction factors were applied (Craig, 1957). Results are given in conventional $\delta^{34}\text{S}$ notation relative to

the Vienna Canon Diablo troilite standard (V-CDT). The reproducibility based on full replicate analyses of internal laboratory standards was ± 0.2 per mil (1σ).

4. Field relationships of the quartz-pyrite veins

The occurrence of quartz veins is a widely recognised, but little described phenomenon in the rocks of the Assynt Terrane (e.g., the presence of quartz veins is noted in Sheraton et al., 1973). Some generally foliation-parallel veins are clearly relatively late features that are closely associated with shearing along Laxfordian shear zones and the development of schistose, phyllosilicate-rich high strain zones (e.g., Beach, 1976; Beacom, 1999). However, the present study has revealed that an earlier, much more widespread and distinctive group of quartz-pyrite veins are present throughout the Assynt Terrane and at least part of the Gruinard Terrane. The distribution of the quartz veins does not seem uniform – they typically occur in clusters cutting the gneisses in regions covering areas of tens to hundreds of square metres, with particularly well-defined groups recognised in the Loch Assynt and Clashnessie regions of the Assynt Terrane, and along the trace of the CSZ (Fig. 1).

The quartz veins typically range in thickness from a few millimetres to several tens of centimetres (e.g., Fig. 2a-e, g), and are relatively straight and continuous features that can be traced for several metres or, less commonly, tens of metres along strike. They have sharply-defined margins, are occasionally anastomosing and sometimes contain inclusions of country-rock or clusters of pink K-feldspar. Pyrite is not found in all of the veins, but where it occurs it is typically either located along the margins as large crystals (>0.5 mm) or as large clusters (>1 cm) of crystals distributed sparsely throughout the veins (e.g., Fig. 2h). In some cases pyrite clusters have been partially to completely oxidised to hematite or limonite, particularly where they have been exposed at the surface for an extended period; this often gives weathered veins a distinctive localised orange-red staining. Within the CSZ, pyrite crystals are also sometimes found in the sheared gneisses surrounding the vein. In isolated road cut exposures, the development of quartz-pyrite veins is additionally associated with a

localised yellow-brown sulphurous weathering of the gneisses, e.g., in roadcuts east of Lochinver (National grid reference NC 1012 2366; Samples BH2 and 5; Table 1).

4.1. Cross-cutting relationships

The quartz-pyrite veins display a consistent set of cross-cutting relationships with other features in the Lewisian Complex. They typically cross-cut the oldest, moderately to shallowly-dipping Badcallian foliations and folds (e.g., Fig. 2a), although in areas where the foliation is particularly intense and of variable orientation (e.g. Clashnessie), the veins may locally be concordant with the local foliation. The veins also consistently cross-cut the steeply-dipping Inverian shear fabrics of the CSZ (e.g., Fig. 2b) and other minor shear zones of this age within the terrane, as well as all observed Scourie dykes (e.g., Fig. 2c). Both veins and dykes are consistently overprinted and reworked by dextral shear fabrics related to the Laxfordian event, including the development of the central part of the CSZ (Attfield 1987; e.g., Fig. 2d). The quartz veins are also post-dated by 'late Laxfordian', epidote-bearing small-scale shear zones and fractures, which exhibit a predominantly sinistral sense of shear (e.g., Fig. 2e, f; see Beacom et al 2001). Many of the larger quartz vein clasts found in the immediately overlying basal units of the Torridonian sandstones are plausibly derived from the basement veins. The quartz-pyrite veins are everywhere cross-cut by gouge-bearing Phanerozoic (post-Cambrian) normal faults (e.g., NC 1020 2360).

Thus the field observations suggest that the quartz-pyrite veins post-date Badcallian structures, the NW-SE trending Inverian fabrics and Scourie dykes. They appear to pre-date all Laxfordian fabrics, 'late Laxfordian' faults, the deposition of the Torridonian sediments and all post-Torridonian deformation episodes (mainly faulting).

4.2. Orientation and kinematics

The orientations of 140 quartz-pyrite veins measured in the Assynt Terrane during the present study are shown in Figures 3a-c, and the sparse lineations found on the veins in Figure 3aii. A rose diagram plot (Fig. 3ai) suggests a predominance of NE-SW strikes with

subordinate NW-SE trends. The regional stereograms (Figs. 3biv-vi & c) better illustrate the rather wider range of vein orientations, with a reasonably strong concentration of planes striking NE-SW and, to a lesser extent NW-SE. Both sets display bimodal dip directions (e.g., NW or SE and NE or SW, respectively; Figs. 3biv-vi & c). These observations suggest a generally multimodal pattern of fracture orientations.

In order to investigate the possible effects on vein orientation of local country rock fabrics and Laxfordian overprinting, the data have been plotted according to the age of the local fabrics they cross-cut or are reworked by (Fig. 3b). In the regions of gneiss dominated by the Badcallian event, both the foliations (Fig. 3bi) and the veins (Fig. 3biv) have large variations in their orientations. The foliation shows a poorly-defined N-S trend dipping shallowly W, whereas the veins show a reasonably strong NE-SW trend, with bimodal dips steeply to the NW and rather more shallowly to the SE. The Inverian foliation has a strong NW-SE trend with generally steep dips (Fig. 3bii), whereas the veins show a strong NE-SW trend with dips mainly being steep and to the NW (Fig. 3bv). Both the Laxfordian foliation and the veins within the Laxfordian fabrics show a strong NW-SE trend and steep dips (Figs. 3biii and vi), reflecting the strong reworking and reorientation of veins into parallelism with those fabrics during overprinting deformation.

The data have also been plotted according to the localities where well-defined clusters of veins are found (Figs. 3ci-vi). The stereoplots for localities such as Clashnessie and Achmelvich areas (Figs. 3ci-ii) show a wide range of orientations whilst the best defined, statistically significant trend is found in the Loch Assynt cluster (Fig. 3cv). Here there is a very well-defined trend striking NE-SW with the majority of veins dipping steeply NW. It may be significant that the pre-vein Badcallian foliation in this area is much weaker compared to areas such as Clashnessie.

The kinematics of the quartz veins are difficult to deduce with any precision. Most of the veins appear to be dilational (Mode 1 tensile) features based on observed offsets of markers in the adjacent wall rocks, i.e., the vein opening directions lie at high angles to the vein walls). A few large veins in the Loch Assynt and Lochinver regions display regular en

Formatted: Font: Not Bold

echelon off-shoots (e.g., Fig. 2g) consistent with some degree of vein-parallel shearing during emplacement (e.g. Peacock & Sanderson 1995). Of the seven veins found with such off-shoots, five indicated a sinistral and two a dextral sense of shear. There does not appear to be any obvious orientation control on the shearing directions, suggesting the shearing may be due to local strain heterogeneities. A few veins ($n = 7$) unaffected by Laxfordian reworking display poorly developed mainly oblique mineral lineations on their outer contacts (Fig. 3a_{ii}).

56. Rhenium-Osmium Geochronology

The total Re and Os abundances of the pyrite samples range from 6.8 to 25.8 ppb (parts per billion) and 298.8 to 660.5 ppt (parts per trillion; Table 1), respectively. The majority of the Os within the samples is radiogenic ^{187}Os ($> 92\%$). Four of the samples possess $> 99\%$ radiogenic ^{187}Os (Table 1). As a result, the $^{187}\text{Re}/^{188}\text{Os}$ values are high to very high (265.6 to 17531), with the accompanying $^{187}\text{Os}/^{188}\text{Os}$ values being very radiogenic (11.04 to 675.2). The predominance of radiogenic ^{187}Os ($^{187}\text{Os}^r$) in the pyrite samples defines them as Low Level Highly Radiogenic (LLHR; Stein et al., 2000; Morelli et al., 2005). To account for the high-correlated uncertainties between the $^{187}\text{Re}/^{188}\text{Os}$ and $^{187}\text{Os}/^{188}\text{Os}$ data we present the latter with the associated uncertainty correlation value, ρ (Ludwig, 1980), and the 2σ calculated uncertainties for $^{187}\text{Re}/^{188}\text{Os}$ and $^{187}\text{Os}/^{188}\text{Os}$ (Table 1). The regression of all the Re-Os data using *Isoplot V. 3.0* (Ludwig, 2003) and the ^{187}Re decay constant (λ) of $1.666 \times 10^{-11} \text{a}^{-1}$ (Smoliar et al., 1996) yields a Model 3 Re-Os age of 2259 ± 61 (2.9 %) Ma, with an initial $^{187}\text{Os}/^{188}\text{Os}$ of 0.9 ± 9.0 (2σ , Mean Squared Weighted Deviates [MSWD] = 22; Fig. 5a). Although the calculated Re-Os age has only a 2.9 % uncertainty, the high MSWD value (22) suggests that the degree of scatter about the regression line is a function of pyrite Re-Os systematics (discussed below). The imprecision of the initial $^{187}\text{Os}/^{188}\text{Os}$ does not permit an accurate evaluation of the origin of the Os in the pyrite, however the initial $^{187}\text{Os}/^{188}\text{Os}$ value, including the uncertainty, can be used to calculate the abundance of

$^{187}\text{Os}^r$ from the total ^{187}Os (common plus radiogenic) in the pyrite samples ($^{187}\text{Os}^{r1}$; Table 1).

The $^{187}\text{Os}^r$ is a product of ^{187}Re decay and model Re-Os dates for each sample can be directly calculated using $t = \ln(^{187}\text{Os}^r / ^{187}\text{Re} + 1) / \lambda$. The model Re-Os dates, with the exception of sample 64.1, all agree - within uncertainty - with the traditional $^{187}\text{Re}/^{188}\text{Os}$ vs $^{187}\text{Os}/^{188}\text{Os}$ isochron age (Table 1; Fig. 5a). One sample from a vein cutting Badcallian gneisses east of Lochinver (64.1; NC 1038, 2249) yields an imprecise model age of 1597.6 ± 1371.2 Ma. Although this date is within uncertainty of the other model ages and the Re-Os isochron age, its nominal age is significantly younger (~800 Ma) than for the other five pyrite samples. As such, sample 64.1 may represent a separate, distinct quartz and pyrite mineralization event. If we consider this to be the case and regress the $^{187}\text{Re}/^{188}\text{Os}$ vs $^{187}\text{Os}/^{188}\text{Os}$ data without sample 64.1, a $^{187}\text{Re}/^{188}\text{Os}$ vs $^{187}\text{Os}/^{188}\text{Os}$ age of 2249 ± 77 Ma, with an initial $^{187}\text{Os}/^{188}\text{Os}$ of 3 ± 13 , is produced (2σ , MSWD = 15; Fig. 5a). This Re-Os isochron age is within uncertainty of that determined from all the Re-Os data, but the degree of scatter about the isochron is reduced (MSWD of 15 vs 22).

Isochron ages can also be determined by the regression of ^{187}Re vs $^{187}\text{Os}^r$ plus their uncertainties. Excluding sample 64.1 for the reasons noted above, the ^{187}Re data together with the $^{187}\text{Os}^r$ values ($^{187}\text{Os}^{r2}$; Table 2) calculated using the initial $^{187}\text{Os}/^{188}\text{Os}$ value (3 ± 13) determined from the $^{187}\text{Re}/^{188}\text{Os}$ vs $^{187}\text{Os}/^{188}\text{Os}$ isochron without sample 64.1 (Fig. 5), a ^{187}Re vs $^{187}\text{Os}^r$ isochron date of 2170 ± 180 Ma is obtained (Fig. 5b, initial $^{187}\text{Os} = 15 \pm 31$ ppt, MSWD = 0.6). We note that with the exception of sample 28 (Lochan Sgeireach) Re-Os model ages calculated using $^{187}\text{Os}^r$ based on the initial $^{187}\text{Os}/^{188}\text{Os}$ value of 3 ± 13 are extremely similar (Table 1). However, sample 28 yields a Model age ~450 Ma younger than an age calculated using the initial of 0.9. Both calculated Model ages have very large uncertainties. This sample possesses the least amount of $^{187}\text{Os}^r$ (~92 ppt – 73%), with its abundance dramatically affected by the initial $^{187}\text{Os}/^{188}\text{Os}$ value (0.9 vs 3; Table 1).

A weighted average of the model Re-Os ages (not including sample 64.1) calculated using a $^{187}\text{Os}^r$ based on the initial $^{187}\text{Os}/^{188}\text{Os}$ value of 3 ± 13 is 2248 ± 38 (MSWD = 0.6;

Fig. 5c). In summary, the ages determined from both the Re-Os isochron methods and the weighted average of the Re-Os model ages are all within uncertainty. We favour using the $^{187}\text{Re}/^{188}\text{Os}$ vs $^{187}\text{Os}/^{188}\text{Os}$ isochron age (without sample 64-1). From this study we consider the majority of the pyrite mineralization and by inference the precipitation the quartz pyrite veins and fracture formation occurred at 2249 ± 77 Ma.

67. Sulphur Isotope Analysis

All the samples from the sulphur isotope analysis yielded high amounts of sulphur (82 to, 97% yield). The $\delta^{34}\text{S}$ from the sulphides ranges from +3.0 to -2.2 per mil. All the samples are slightly enriched in ^{34}S relative to 0 per mil, with the exception of sample 64.1, which has a slightly depleted value of -2.2. This may suggest a slightly different source of the sulphur for sample 64.1, and coupled with the Re-Os data may support a distinct quartz and pyrite mineralization event from the other five samples. The range in the $\delta^{34}\text{S}$ values (+3.0 and -2.2) encompasses that of the primitive mantle (Rollinson, 1993). The results therefore suggest that the sulphur in the pyrite is most likely derived from a source not isotopically fractionated from the primitive mantle valuesource.

75. Microstructural textures and inferred deformation mechanisms

75.1. Microstructural textures within quartz-pyrite veins

The quartz-pyrite veins display an array of deformation textures suggesting that they have experienced a complex history of deformation at different temperatures and pressures. A number of overprinting relationships are seen which can be related to the relative chronology of events seen in the field. The deformation textures are described below with reference to the age of the country rock fabric which the veins either cross-cut or are overprinted by.

75.1.1 Veins crosscutting Badcallian structures

Despite modest amounts of grain-scale deformation, the veins cross-cutting Badcallian gneisses (e.g., Fig. 2a, e) preserve a diverse range of deformation microstructures. The most deformed examples contain large quartz crystals (> 1mm, but typically 3 – 7mm) that show sweeping undulose extinction and have highly lobate grain boundaries as a result of grain boundary migration processes during recrystallisation (Stipp et al., 2002). Chessboard subgrains (e.g. Fig. 4a) within quartz crystals are also common and form in response to the migration of dislocations within the crystal lattice into subgrain walls during recrystallisation (e.g. Passchier and Trouw, 2005).

The least plastically deformed veins cutting Badcallian foliation are found on the shores of Loch Assynt (e.g., Figs. 2e, g). The quartz crystals within these veins display undulose extinction, whilst some larger grains contain deformation lamellae, which are zones of differently orientated crystal lattice separated by dislocations. Grain boundaries have undergone small-scale bulging during recrystallisation and small grains (<100µm) have developed within the bulges and along the deformation lamellae (e.g., Fig. 4b).

Overall, the range of deformation microstructures observed in the quartz veins cutting Badcallian gneisses suggests that they experienced small amounts of crystal plastic deformation under moderate temperature (400 - 500°C) conditions. The veins on the shore of Loch Assynt locally preserve rather lower temperatures textures (perhaps as low as 300°C) and/or higher strain rate conditions. This may be the result of 'late Laxfordian' deformation associated with slip on the Loch Assynt Fault (e.g., like the structures shown in Figs. 2e, f), to which they are proximal.

7.1.2 Veins cross-cutting Inverian structures

Veins emplaced into Lewisian gneisses reworked by Inverian deformation (e.g., Fig. 2b) also show little obvious deformation at outcrop scale. A range of deformation microstructures are preserved, including undulose extinction, deformation lamellae, new grain growth along crystal boundaries, subgrain development and the development of lobate grain boundaries. These are indicative of recrystallisation under low to moderate temperatures (350 - 500°C)

and high to moderate strain rates. Some veins contain large (>2mm) quartz crystals with lobate boundaries, formed by grain boundary migration under moderate temperatures and strain rates, which show grain boundary bulging and the development of new, small grains (<250µm) within the bulges, particularly at triple-point grain boundaries (Fig. 4c). These structures are typical of recrystallisation under somewhat lower temperatures (300 - 400°C), and may indicate a lower temperature event. There is little evidence for this event within the veins emplaced into Badcallian gneisses, and it may be that it is related to localised later deformation and/or fluid flow restricted to the Inverian shear zones immediately following vein emplacement. Alternatively, it may be a weak manifestation of Laxfordian deformation given the regionally observed coincidence of Inverian and Laxfordian reworking (e.g. Attfield 1987).

7.1.3 Veins overprinted by Laxfordian structures

The veins emplaced within the Laxfordian part of the CSZ (e.g., Fig. 2d) have been heavily reworked at outcrop scale. Many of the grain-scale textures resulting from the recrystallisation of quartz are similar to those seen in the veins which were emplaced into gneisses with Badcallian and Inverian foliations, but the finite strains are much higher. In most veins, larger quartz crystals (>2mm) show sweeping undulose extinction, deformation lamellae, subgrain development and lobate grain boundaries. These microstructures indicate deformation under moderate temperatures (350 - 500°C) and strain rates. Relict S-C' mylonite fabrics (e.g. Berthé et al. 1979; Snoke et al. 1998) are preserved in the most highly deformed veins (e.g., Fig. 4d). Sub-parallel fine-grained (<100 µm) bands of feldspar, muscovite and chlorite define the C-surfaces which are enclosed by polygonal quartz aggregate (with grains sizes 0.5 – 3 mm). Quartz grain boundaries are often pinned by aligned micas and some fine aligned grains are completely enclosed by much larger, undeformed quartz grains (Fig. 4d). These fabrics are typical indicators of significant secondary grain growth under elevated temperature conditions (e.g., Vernon 1976; Passchier and Trouw, 2005).

75.1.4 Pyrite microstructural relationships

Pyrite occurs in a variety of forms in the veins of the Assynt Terrane. Some samples contain large clusters of pyrite crystals up to 1.5cm in across (e.g., Fig. 2h) which are intimately intergrown with quartz (e.g., Figs 4e, f). SEM images reveal the partial alteration of pyrite grains to iron oxides along grain margins and fractures within some large pyrite clusters (e.g., Fig. 4g, h). Small (<1mm) pyrite clusters are also associated with the mylonitized quartz veins within the CSZ. There is little evidence for significant deformation of the pyrite grains during recrystallization of the surrounding quartz aggregates even in cases where the intensity of finite plastic strain is high.

75.1.5 Summary

The microstructural evidence from the veins suggests that most of the pyrite initially crystallised at the same time as the quartz and that it is therefore a primary mineral phase. The veins then experienced very modest amounts of deformation and recrystallisation during a moderate temperature (350 - 500°C) and low strain rate strain rate event felt throughout most of the Assynt Terrane. Given the similarity in quartz microstructures and interpreted palaeotemperatures with the more highly deformed veins in the CSZ, it seems most likely that the bulk of the modest deformations recorded here are also Laxfordian to 'late Laxfordian' in age (ca. 1780-1400). Laxfordian deformation, especially within the CSZ, resulted in the formation of mylonitic fabrics within the veins under mostly moderate temperatures (350 - 500°C). There may also have been some limited remobilisation and re-precipitation of pyrite related to fluid flow both within the veins and the adjacent sheared gneisses.

8. Discussion:

The Re-Os isochron age obtained from the majority of the quartz-pyrite veins (2249 ± 77 Ma) is consistent with our current understanding of the broad ages of regional

1
2
3 475 tectonometamorphic episodes in the Lewisian Complex (Fig. 6). Specifically, they cross cut
4
5 476 older Badcallian (*ca.* 2760 or 2480 Ma) and Inverian (*ca.* 2400-2480 Ma) fabrics and are
6
7 477 overprinted/reworked by younger Laxfordian (1790-1660 Ma) structures. The latter suggests
8
9 478 that the Re-Os systematics were not appreciably disturbed by structural reworking and the
10
11 479 upper greenschist conditions associated with the Laxfordian event.

12 480 The most recent U-Pb geochronology shows that intrusion of the Scourie dykes
13
14 481 predominantly occurred at 2391 – 2404 Ma, with moderately younger ages (2367 – 2372
15
16 482 Ma) at the SW edge of the Assynt Terrane (Davies and Heaman, 2014⁴³). The *ca.* 2250 Ma
17
18 483 age for the quartz-pyrite veins falls within the range of ages obtained from the NW-SE
19
20 484 trending Scourie dyke swarm across the entire Lewisian Complex (Fig. 6; 2418 Ma to 1991
21
22 485 Ma; Chapman 1979; Heaman and Tarney, 1989; Cohen et al., 1988; Waters et al., 1990;
23 486 Davies and Heaman, 2014⁴³). These studies suggest two main episodes of dyke intrusion at
24
25 487 *ca.* 2418 Ma and 1992 Ma (Fig. 6; Davies and Heaman, 2014⁴³), with distinct mantle sources
26
27 488 exploited during each event (Cartwright and Valley, 1991). The idea that there are multiple
28
29 489 episodes of 'Scourie dyke's intrusion is consistent with some geological field relationships. It
30
31 490 is known, for example, in the southern region of the Lewisian Complex that some 'Scourie
32 491 dykes' cut the Loch Maree Group metasediments and metavolcanics, which were thought to
33
34 492 have formed in oceanic basins and accreted to the continental crust through subduction
35
36 493 between 2000 and 1900 Ma (Park et al., 2001).

37
38 494 All the quartz-pyrite veins observed during the present study seen in the Assynt
39
40 495 Terrane cross-cut Scourie dykes, although this does not preclude the possibility that
41
42 496 regionally there may be some dykes that are younger. However, the Re-Os pyrite dating of
43 497 the veins at *ca.* 2250 Ma suggests a complex polyphase early Palaeoproterozoic tectonic
44
45 498 history of the Lewisian complex (Fig. 6). Veins form by the precipitation of minerals in dilating
46
47 499 hydrofractures and their regional development in clusters and swarms are indicative of
48
49 500 significant phase of ~~crustal-scale~~ fluid flow in the crust (e.g., Sibson, 1996 and references
50
51 501 therein). The simplest types of vein are Mode 1 fractures which open in the direction of the
52
53 502 minimum principle stress and have strike orientations perpendicular to it (e.g., Peacock &
54
55
56
57
58
59
60
61
62
63
64
65

Formatted: Font: Italic

Formatted: Font: Italic

Formatted: Font: Italic

Formatted: Font: Italic

Formatted: Font: Italic

Mann, 2005). Most of the veins in the Assynt Terrane appear on the basis of their field relationships to be Mode I features (e.g. Fig. 2a). If so, the prevalence of NE-SW strikes (e.g., Figs. 1, 3ai) implies a NW-SE opening direction, although the veins show a wide range of other orientations (Figs. 3b,c) which are attributed to a number of factors: the presence of highly variable foliation in strongly banded gneisses; the presence of pre-existing fractures, or to the reworking of veins by Laxfordian fabrics.

The pre-Laxfordian NE-SW orientation and inferred NW-SE opening directions of the quartz-pyrite veins lie almost orthogonal to the regional NW-SE orientation – and inferred NE-SW extension direction – of the Scourie dykes. If there are multiple episodes of Scourie dykes on a regional scale, with some pre-dating and some post-dating the quartz-pyrite veins, this implies that there were significant changes in the orientation of regional stress vectors in the 500 Ma period between 2400 and 1900 Ma (Fig. 6). Note, however, that in common with the Scourie dykes, the sulphur isotopic analysis of the quartz-pyrite veins is suggestive of a source not isotopically fractionated from the primitive mantle derivation ~~Note, however, that in common with the Scourie dykes, the sulphur isotopic analysis of the quartz-pyrite veins is suggestive of a primitive mantle derivation~~ (Rollinson, 1993).

Although ~~The~~ Re-Os ~~model aged data for~~ sample 64.1 provide a highly imprecise model age (1597.6 ± 1356 Ma) its nominal age is considerably younger than the model ages for the other samples (2198.5 – 2328.7 Ma), and, in addition, ~~has a very large uncertainty as well as~~ the lowest Os abundance of (242.8 ± 33.9 ppb) of all the samples; ~~it~~. Furthermore, sample 64.1 is also the only sample with a depleted $\delta^{34}\text{S}$ value (-2.2). Although this value could indicate that the sulphur source is not isotopically fractionated from the primitive mantle ~~value is derived from the primitive mantle~~, like the other samples, it may be that the sulphur ~~uride~~ within the ~~vein-pyrite~~ has a slightly different origin to that found within other veins, or that it may have been disturbed following emplacement, perhaps related to a later phase of 'late Laxfordian' brittle fracture fractures and fluid ingress. Further work and dating is required to verify the age obtained and better constrain the geological and geochronological significance of this younger age.

86.1. Implications for terrane models

Dating of the TTG protoliths suggests that the gneisses of the Gruinard Terrane are at least 100 Ma younger than those of the Assynt Terrane and underwent granulite metamorphism at 2730 Ma (Love et al., 2004; Park, 2005). Thus they are thought to belong to different and separate Archaean terrane which amalgamated along the Strathan Line, south of Lochinver, during Inverian folding and retrogression (Fig. 1, Love et al., 2004). The presence of post-Inverian quartz-pyrite veins within both the Assynt and Gruinard Terranes is consistent with this proposal.

The amphibolite-facies gneisses of the Rhiconich Terrane to the north have yielded protolith ages of 2840-2800 Ma and a record magmatism at 2680 Ma (Kinny and Friend, 1997), but there is no apparent evidence of metamorphism at ca. 2780 Ma. This led Friend and Kinny (2001) to suggest that the Assynt and Rhiconich Terranes were separate Archaean crustal blocks of differing age and early history that were only finally juxtaposed by a major episode of shearing during the along the Laxfordian Shear Zone at ca. 1750 Ma (Fig. 1). This seems consistent with the apparent absence of ca. 2250 Ma quartz-pyrite veins in the Rhiconich Terrane. However, recent fieldwork and dating by Goodenough et al. (2010; 2013) has found evidence that the Laxford Shear Zone initially formed as an Inverian structure, pre-dating the intrusion of a regional suite of arc-related granitic sheets ca. 1880 Ma into both the Assynt and Rhiconich Terranes. These granites are then overprinted by the main Laxfordian deformation and associated amphibolite-facies metamorphism, which ranges from 1790-1670 Ma (Corfu et al., 1994; Kinny and Friend, 1997; Love et al., 2010). In this case the absence of the quartz-pyrite veins to the north of the Laxford Shear Zone is perhaps consistent with significant Laxfordian-age reactivation leading to final juxtaposition of the two terranes.

97. Conclusions

Formatted: Font: Italic

Formatted: Font: Italic

A hitherto unrecognised set of quartz-pyrite veins have been identified in the Assynt and Gruinard terranes of the Lewisian complex. The veins consistently cross-cut Badcallian and Inverian structures in the gneisses, as well as (at least) the majority of Scourie dykes. They are reworked during Laxfordian shearing events and are also cross cut by a range of later brittle faulting events. The dominant strike direction of the quartz-pyrite veins suggests emplacement during a regional NW-SE extension of the crust, whilst sulphur isotope analyses of the pyrites ~~suggest are consistent with~~ a primitive mantle origin for the fluids.

The Re-Os date of 2249 ± 77 Ma for the pyrite within the veins is consistent with the field relationships and other known geochronological constraints in the Lewisian Complex. Both the Scourie dykes and quartz-pyrite veins are most likely developed as Mode I tensile fractures, but their almost orthogonal present day orientations suggests that whilst the dykes were emplaced during two or more periods of NE-SW crustal extension and associated mafic magmatism ca. 1900-2400 Ma, the quartz-pyrite mineralization ca. 2250 Ma occurred during an intervening phase of NW-SE extension.

The presence of the quartz-pyrite veins in both the Assynt and Gruinard terranes confirms their amalgamation prior to ca. 2250 Ma, most likely during the Inverian. The apparent absence of the veins in the Rhiconich Terrane suggests it may not have been finally amalgamated with the Assynt and Gruinard terranes until the Laxfordian. More generally, this study demonstrates the potential value of the Re-Os technique as a means of dating sulphide mineralisation events in continental basement terrains worldwide.

Acknowledgements

This research was supported, in part, by a student grant from the Geological Society of London to RV. Rob Strachan, ~~an anonymous reviewer and Randy Parrish are-is~~ thanked for their constructive comments and suggestions ~~on earlier versions of this manuscript as~~ reviewers.

References

Formatted: Font: Italic

Formatted: Font: Italic

Formatted: Font: Italic

- Attfield, P., 1987. The structural history of the Canisp Shear Zone, *In: Park, R.G. & Tarney, J. (eds), The early Precambrian rocks of Scotland and related rocks of Greenland*, Department of Geology, Keele, 165-174.
- Beach, A., 1976. The interrelations of fluid transport, deformation, geochemistry and heat flow in early Proterozoic shear zones in the Lewisian complex, *Philosophical Transactions Royal Society London A*, **280**, 569-604.
- Beacom, L.E., 1999. *The Kinematic Evolution of Reactivated and Non-Reactivated Faults in Basement Rocks, NW Scotland*, Unpublished PhD thesis, Queens University, Belfast.
- Beacom, L.E., Holdsworth, R.E., McCaffrey, K.J.W. & Anderson, T.B., 2001. A quantitative study of the influence of pre-existing compositional and fabric heterogeneities upon fracture-zone development during basement reaction, *In: Holdsworth, R.E., Strachan, R.A., Magloughlin, J.F. & Knipe, R.J. (eds). The Nature and Tectonic Significance of Fault Zone Weakening*, Geological Society Special Publications, London, **186**, 195-211.
- Berthé, D., Choukroune, P., and Jegouzo, P., 1979. Orthogneiss, mylonite and non coaxial deformation of granites: the example of the South Armorican shear zone. *Journal of Structural Geology*, **1**, 31-43
- Cameron, E.M., 1994. Depletion of gold and LILE in the lower crust: Lewisian Complex, Scotland, *Journal of the Geological Society*, **151**, 747-754.
- Cartwright, I. & Valley, J.W. 1991. Low-¹⁸O Scourie dike magmas from the Lewisian complex, northwestern Scotland. *Geology* **19**, 578-581.
- Chapman, H.J. 1979. 2,390 Myr Rb-Sr whole-rock age for the Scourie dykes of north-west Scotland. *Nature*, **277**, 642-3.
- Chattopadhyay, A., Holdsworth, R.E., McCaffrey, K.J.W. & Wilson, R.W. 2010. Recording and Analyzing Geospatially Accurate Structural Data through 'Digital Mapping' Technique: A Case Study from the Canisp Shear Zone, NW Scotland. *Journal of the Geological Society of India*, **75**, 43-59.
- Cohen, A.S., Waters, F.G., O'Nions, R.K. & O'Hara, M.J., 1988. A precise crystallisation age for the Scourie Dykes, and a new chronology for crustal development in north-west Scotland. *Chemical Geology*, **70**, 19.
- Coleman, M.L. & Moore, M.P., 1978. Direct Reduction of Sulfates to Sulfur Dioxide for Isotopic Analysis, *Analytical Chemical Society*, **50**, 1594-1595.
- Corfu, F., Heaman, L.M. & Rogers, G. 1994: Polymetamorphic evolution of the Lewisian complex, NW Scotland, as recorded by U-Pb isotopic compositions of zircon, titanite and rutile. *Contributions to Mineralogy and Petrology*, **117**, 215-228.
- Coward, M.P. & Park, R.G., 1987. The role of mid-crustal shear zones in the Early Proterozoic evolution of the Lewisian, *In: Park, R.G. & Tarney, J. (eds), Evolution of the Lewisian and Comparable Precambrian High Grade Terrains*, Geological Society Special Publications, London, **27**, 127-138.
- Craig, H., 1957. Isotopic standards for carbon and oxygen and correction factors for mass-spectrometric analysis of carbon dioxide, *Geochimica et Cosmochimica*, **12**, 133-149.

Davies, J.H.F.L. & Heaman, L.M., 2014⁴³, New U-Pb baddeleyite and zircon ages for the Scourie dyke swarm: A long-lived large igneous province with implications for the Paleoproterozoic evolution of NW Scotland. *Precambrian Research*, [In Press, in review](#).

Dickinson, B.B. & Watson, J., 1976. Variations in crustal level and geothermal gradient during the evolution of the Lewisian Complex of Northwest Scotland, *Precambrian Research*, **3**, 363-374.

Droop, G.T.R., Fernandes, L.A.D. & Shaw, S., 1989. Laxfordian metamorphic conditions of the Palaeoproterozoic Loch Maree Group, Lewisian Complex, NW Scotland, *Scottish Journal of Geology*, **35**, 31-50.

Finlay, A. J., Selby, D., Osborne, M., 2011. Re-Os geochronology and fingerprinting of United Kingdom Atlantic Margin oil: Temporal Implications for regional petroleum systems, *Geology*, **39**, 475-478.

Friend, C.R.L. & Kinny, P.D. 1995. New evidence for the protolith ages of Lewisian granulites, northwest Scotland. *Geology*, **23**, 1027-1030.

Friend, C.R.L. & Kinny, P.D. 2001. A reappraisal of the Lewisian Gneiss Complex: geochronological evidence for its tectonic assembly from disparate terranes in the Proterozoic, *Contribution to Mineralogy and Petrology*, **142**, 198-218.

~~Floyd, P.A., Winchester, J.A. & Park, R.G., 1989. Geochemistry and Tectonic Setting of Lewisian Clastic Metasediments from the Early Proterozoic Loch Maree Group of Gairloch, NW Scotland, *Precambrian Research*, **45**, 203-214.~~

Goodenough, K.M., Park, R.G., Krabbendam, M., Myers, J.S., Wheeler, J., Loughlin, S., Crowley, Q., L.F.C.R., Beach, A., Kinny, P.D., Graham, R., 2010. The Laxford Shear Zone: an end-Archaean terrane boundary? In: Law, R., Butler, R.W.H., Holdsworth, R.E., Krabbendam, M., Strachan, R. (eds.), *Continental Tectonics and Mountain Building*. Geological Society Special Publication, **335**, 103-120.

Goodenough, K.M., Crowley, Q.G., Krabbendam, M. & Parry, S.E. 2013. New U-Pb age constraints for the Laxford Shear Zone, NW Scotland: Evidence for tectono-magmatic processes associated with the formation of a Palaeoproterozoic supercontinent. *Precambrian Research*, **233**, 1-19.

Gramlich, J.W., Murphy, T.J., Garner, E.L. & Shields, W.R., 1973. Absolute isotopic abundance ratio and atomic weight of a reference sample of rhenium, *Journal of Research of the National Bureau of Standards*, **77A**, 691-698.

Hamilton, P.J., Evensen, N.M., O'Nions, R.K., Tarney, J., 1979. Sm-Nd systematics of Lewisian gneisses: implications for the origin of granulites. *Nature*, **277**, 25-28.

Heaman, L.M. & Tarney, J., 1989. U-Pb baddeleyite ages for the Scourie dyke swarm, Scotland: evidence for two distinct intrusion events, *Nature*, **340**, 705-708.

~~Hirth, G. & Tullis, J., 1992. Dislocation creep regimes in quartz aggregates, *Journal of Structural Geology*, **14**, 145-159.~~

Jensen, L.N., 1984. Quartz microfabric of the Laxfordian Canisp Shear Zone, NW Scotland, *Journal of Structural Geology*, **6**, 293-302.

Kinny, P., Friend, C., 1997. U-Pb isotopic evidence for the accretion of different crustal blocks to form the Lewisian Complex of Northwest Scotland. *Contributions to Mineralogy and Petrology*, **129**, 326–340.

Kinny, P.D., Friend, C.R.L. & Love, G.L., 2005. Proposal for a terrane-based nomenclature for the Lewisian Gneiss Complex of NW Scotland, *Journal of the Geological Society*, **162**, 175–186.

Love, G.J.L, Kinny, P.D. & Friend, C.R.L., 2004. Timing of magmatism and metamorphism in the Gruinard Bay area of the Lewisian Gneiss Complex: comparisons with the Assynt Terrane and implications for terrane accretion, *Contributions to Mineralogy and Petrology*, **146**, 620–636.

Love, G.J., Friend, C.R.L., Kinny, P.D., 2010. Palaeoproterozoic terrane assembly in the Lewisian Gneiss Complex on the Scottish mainland, south of Gruinard Bay: SHRIMP U–Pb zircon evidence. *Precambrian Research*, **183**, 89–111.

Ludwig, K.R., 1980, Calculation of uncertainties of U-Pb isotope data: *Earth and Planetary Science Letters*, **46**, 212–220.

Ludwig, K.R., 2003, Isoplot/Ex, version 3: A geochronological toolkit for Microsoft Excel: Berkeley, CA, Geochronology Center Berkeley.

Moorbath, S., Welke, H., Gale, N., 1969. The significance of lead isotope studies in ancient, high-grade metamorphic basement complexes, as exemplified by the Lewisian rocks of Northwest Scotland. *Earth and Planetary Science Letters*, **6**, 245–256.

Morelli, R.M., Creaser, R.A., Selby, D., Kontak, D.J. and Horne, R.J., 2005, Rhenium-Osmium arsenopyrite geochronology of Meguma Group gold deposits, Meguma terrane, Nova Scotia, Canada: Evidence for multiple gold mineralizing events, *Economic Geology*, **100**, 1229–1242.

O'Hara, M.J. 1961. Petrology of the Scourie Dyke, Sutherland. *Mineralogical Magazine*, **32**, 848–865.

Park, R.G., 1970. Observations on Lewisian chronology. *Scottish Journal of Geology*, **6**, 379–399.

Park, R.G., 2005. The Lewisian terrane model: a review, *Scottish Journal of Geology*, **41**, 105–118.

Park., R.G. & Tarney, J., 1987. The Lewisian Complex: a typical Precambrian high-grade terrane?, In: Park, R.G. & Tarney, J. (eds), *Evolution of the Lewisian and Comparable Precambrian High Grade Terranes*, Geological Society, London, 13–26.

Park, R.G., Cliff, R.A., Fettes, D.J., Stewart A.D., 1994. Precambrian rocks in northwest Scotland west of the Moine Thrust: the Lewisian Complex and the Totridonian. In: W. Gibbons and A.L. Harris (Editors), *A Revised Correlation of Precambrian Rocks in the British Isles*. Geological Society of London Special Report, **22**, 6–22.
~~Park et al. 1994.~~

Park, R.G, Tarney, J. & Connelly, J.N., 2001. The Loch Maree Group: Palaeoproterozoic subduction-accretion complex in the Lewisian of NW Scotland, *Precambrian Research*, **105**, 205–226.

Formatted: Font: Italic

Formatted: Font: Bold

- Park, R.G., Stewart, A.D. & Wright, D.T. 2002. The Hebridean Terrane. In: Trewin, N.H. (ed) *The Geology of Scotland*. Geological Society, London, 45-80.
- Passchier, C.W. & Trouw, R.A.J., 2005. *Micro-Tectonics*, Springer Berlin Heidelberg, New York, 25-66.
- Peacock, D.C.P. & Mann, A., 2005. Evaluation of the controls on fracturing in reservoir rocks, *Journal of Petroleum Geology*, **28**, 385-396.
- Peacock, D.C.P. & Sanderson, D.J. 1995. Pull-aparts, shear fractures and pressure solution. *Tectonophysics*, 241, (1-2), 1-13.
- Rollinson, H., 1993. *Using Geochemical Data: evaluation, presentation, interpretation*, Longman Group UK Ltd, Harlow, 303-306.
- Selby, D., Kelley, K.D., Hitzman, M.W. & Zieg, J., 2009. Re-Os sulphide (Bornite, Chalcopyrite, and Pyrite) systematic of the Carbonate-hosted copper deposits at Ruby Creek, Southern Brooks Range, Alaska, *Economic Geology*, **104**, 437-444.
- Sibson, R.H. 1996. Structural permeability of fluid-driven fault-fracture meshes. *Journal of Structural Geology*, **18**, 1031-1042.
- Sheraton, J.W., Tarney, J., Wheatley, T.J. & Wright, A.E., 1973. The structural history of the Assynt district, In: Park, R.G. & Tarney, J. (eds), *The early Precambrian rocks of Scotland and related rocks of Greenland*, Department of Geology, Keele, 13-30.
- Smoliar, M.I., Walker, R.J., & Morgan, J.W., 1996. Re-Os isotope constraints on the age of Group IIA, IIIA, IVA, and IVB iron meteorites, *Science*, **271**, 1099-1102.
- Snoke, A.W., Tullis, J. and Todd, V.R., 1998. *Fault-related Rocks*. Princeton University Press, Princeton New Jersey, New Jersey, 617 pp.
- Stein, H.J., Morgan, J.W. & Schersten, A., 2000. Re-Os of Low-Level Highly Radiogenic (LLHR) Sulphides: The Hurnas Gold Deposit, Southwest Sweden, Records Continental-Scale Tectonic Events, *Economic Geology*, **95**, 1657-1671.
- Stipp, M., Stunitz, H., Heilbronner, R. & Schmid, S.M., 2002. The eastern Tonale fault zone: a 'natural laboratory' for crystal plastic deformation of quartz over a temperature range from 250 to 700°C, *Journal of Structural Geology*, **24**, 1861-1884.
- Sutton, J. & Watson, J., 1951. The pre-Torridonian metamorphic history of the Loch Torridon and Scourie areas in the north-west Highlands, and its bearing on the chronological classification of the Lewisian, *Quarterly Journal of the Geological Society*, **106**, 241-307.
- Tarney, J., 1973. The Scourie dyke suite and the nature of the Inverian event in Assynt, In: Park, R.G. & Tarney, J. (eds), *The early Precambrian rocks of Scotland and related rocks of Greenland*, Department of Geology, Keele, 31-44.
- Vernon, R.H. 1976. *Metamorphic Processes: Reactions and Microstructure Development*. George Allen & Unwin, pp 247.
- Waters, F.G., Cohen, A.S., O'Nions, R.K. & O'Hara, M.J., 1990. Development of Archaean lithosphere deduced from chronology and isotope chemistry of Scourie Dykes, *Earth and Planetary Science Letters*, **97**, 241-255.

Wheeler, J., Park, R.G., Rollinson, H.R. & Beach, A., 2010. The Lewisian Complex: insights into deep crustal evolution, In: Law, R.D., Butler, R.W., Holdsworth, R.E., Krabbendam, M. & Strachan, R.A. (eds), *Continental Tectonics and Mountain Buildings: The Legacy of Peach and Horne*, Geological Society, London, Special Publications, **335**, 51-79.

Wilkinson, J.J. & Wyre, S.L., 2005. Ore-Forming Processes in Irish-Type Carbonate-hosted Zn-Pb Deposits: Evidence from Mineralogy, Chemistry, and Isotopic Composition of Sulphides at the Lisheen Mine. *Economic Geology*, **100**, 63-86.

~~Wynn, T.J., 1995. Deformation in the mid to lower continental crust: analogues from Proterozoic shear zones in NW Scotland, In: Coward, M.P. & Ries, A.C. (eds), *Early Precambrian Processes*, Geological Society, London, Special Publications, **95**, 225-241.~~

Zhu, X.K., O'Nions, R.K., Belshaw, N.S., Gibb, A.J., 1997. Lewisian crustal history from in situ SIMS mineral chronometry and related metamorphic textures. *Chemical Geology*, **136**, 205-218.

Figure Captions

Figure 1) Highly simplified geological map showing the location and orientations of the quartz vein clusters (i-vi) studied within the Assynt Terrane of the Lewisian Complex. Note that this is not an exhaustive assessment of all quartz veins present in the Assynt Terrane, i.e. there may be many more clusters than are shown here. Inset map shows general location in Scotland and main Lewisian Complex terranes discussed in this paper.

Figure 2) Field relationships of quartz-pyrite veins. a) NE-SW vein cross-cutting shallowly-NW-dipping Badcallian foliation near Clashnessie (NC 0855 3102). Note offset of layers across vein indicating Mode I tensile opening (arrows); b) NE-SW vein (below hammer) cross-cutting steep NW-SE Inverian foliation in Canisp Shear Zone (NC 0521 2593); c) NE-SW vein cross-cutting Scourie dyke on the shore of Loch Assynt (NC 2135 2510); d) NW-SE vein folded and reworked by Laxfordian fabrics, Canisp Shear Zone (NC 0515 2620); e) NE-SW vein cut and offset 10cm by NW-SE sinistral brittle fault in Badcallian gneisses close to the trace of the Loch Assynt Fault (NC 2110 2517); f) En echelon tensile fractures filled with epidote indicating sinistral shear in Badcallian gneisses close to the trace of the Loch Assynt Fault (NC 2110 2517); g) ENE-WSW vein with en-echelon off-shoots, indicating a small component of sinistral shear parallel to the vein margins (NC 2135 2510); h) Large pyrite cluster within a quartz vein (NC1038 2249). Note fracturing of pyrite and characteristic iron

oxide staining.

Figure 3) Orientation data for the regional quartz-pyrite vein suite. a) i) Rose diagram of vein trends for the entire Assynt Terrane (for locality-based versions, see Fig. 1), ii) lower hemisphere equal-area stereoplot of veins with lineated margins; b) Equal area stereoplots of gneiss foliations (i-iii) and of associated veins from each locality (iv-vi) grouped according to the inferred age of the wall rock fabric; c) Equal area stereoplots of quartz vein clusters measured in the six localities (i-vi) shown in Fig 1.

Figure 4) Representative microstructures of quartz-pyrite veins viewed using optical microscope and FESEM. a) Chess-board extinction in large quartz crystals from vein cutting Badcallian gneisses at Kylesku; b) New grains forming along grain boundaries and deformation lamellae, reflecting slightly lower temperature overprint in vein located close to the trace of the Loch Assynt Fault; c) Development of new grains at triple junction grain boundaries overprinting higher temperature deformation features in vein cutting Inverian fabrics near Lochinver; d) Recrystallised S-C fabric in highly sheared veing from the Laxfordian central part of the Canisp Shear Zone, e) Quartz intergrown with within blocky pyrite cluster; f) Intricate intergrowths of pyrite and quartz from vein cutting Scourie dyke at Loch Assynt; g) BSEM image of smooth pyrite (light grey) intergrown with quartz (dark grey) from the same sample as f). The radial fibrous material is iron oxide replacing pyrite; h) Alteration of pyrite (bright grey) along fractures to iron oxides (darker mottled greys), Sample 64.1 (see text for details). Note that all the optical micrographs are cross-polar views.

Figure 5) Re-Os data for the pyrite from the quartz-pyrite veins. A) $^{187}\text{Re}/^{188}\text{Os}$ and $^{187}\text{Os}/^{188}\text{Os}$ plot for all samples and all samples minus sample 64.1; B) ^{187}Re vs $^{187}\text{Os}^r$ plot, with the $^{187}\text{Os}^r$ data calculated using an initial of 3 ± 13 ; C) Weighted average of Re-Os model ages, with the model ages calculated using an initial of 3 ± 13 . See text for discussion.

Figure 6) The chronology of events during the Archaean to Proterozoic in the Assynt

Terrane, showing the range of possible Scourie dyke episodes and the vein emplacement period ascertained during the present study.

Table Caption

Table 1) Re-Os and S isotope data for pyrite from quartz veins in the Lewisian Complex, NW

Scotland. All uncertainties are reported at the 2s level, $^{187}\text{Os}/^{188}\text{Os}$ uncertainties reported at 2SE; all data are blank corrected, blanks for Re and Os were 2.7 ± 1.1 and 0.40 ± 0.42 pg, respectively, with an average $^{187}\text{Os}/^{188}\text{Os}$ value of 0.37 ± 0.17 (1SD, $n = 2$). All uncertainties are determined through the full propagation of uncertainties of the Re and Os mass spectrometer measurements, blank abundances and isotopic compositions, spike calibrations, and reproducibility of standard Re and Os isotopic values. $^{187}\text{Os}^r$ presented are calculated using initial $^{187}\text{Os}/^{188}\text{Os}$, plus its uncertainty, from regression of data using $^{187}\text{Re}/^{188}\text{Os}$ vs. $^{187}\text{Os}/^{188}\text{Os}$ isochron plot; rho is the error correlation.

1 = ^{187}Osr determined from an initial $^{187}\text{Os}/^{188}\text{Os}$ of 0.9 ± 9.0 (Fig. 5A).

2 = $^{187}\text{Os}^r$ determined from an initial $^{187}\text{Os}/^{188}\text{Os}$ of 3 ± 13 (Fig. 5A). With the exception of sample RO297-3/28, the calculated % $^{187}\text{Os}^r$ is very similar using either initial $^{187}\text{Os}/^{188}\text{Os}$ values of 0.9 ± 9.0 or 3 ± 13 . For sample RO297-3/28 the % ^{187}Osr decreases to ~72.8% using an initial $^{187}\text{Os}/^{188}\text{Os}$ value of 3 ± 13 . A model age can be directly calculated using

$$^{187}\text{Os}^r/^{187}\text{Re} = e^{t\lambda} - 1$$

3 = Model age determined using an initial $^{187}\text{Os}/^{188}\text{Os}$ value of 0.9 ± 9.0 (Fig. 5A).

4 = Model age determined using an initial $^{187}\text{Os}/^{188}\text{Os}$ value of 3 ± 13 (Fig. 5A).

5 = The reproducibility based on full replicate analyses of internal laboratory standards was ± 0.2 per mil (1 σ).

Formatted: Superscript

Formatted: Superscript

Formatted: Superscript

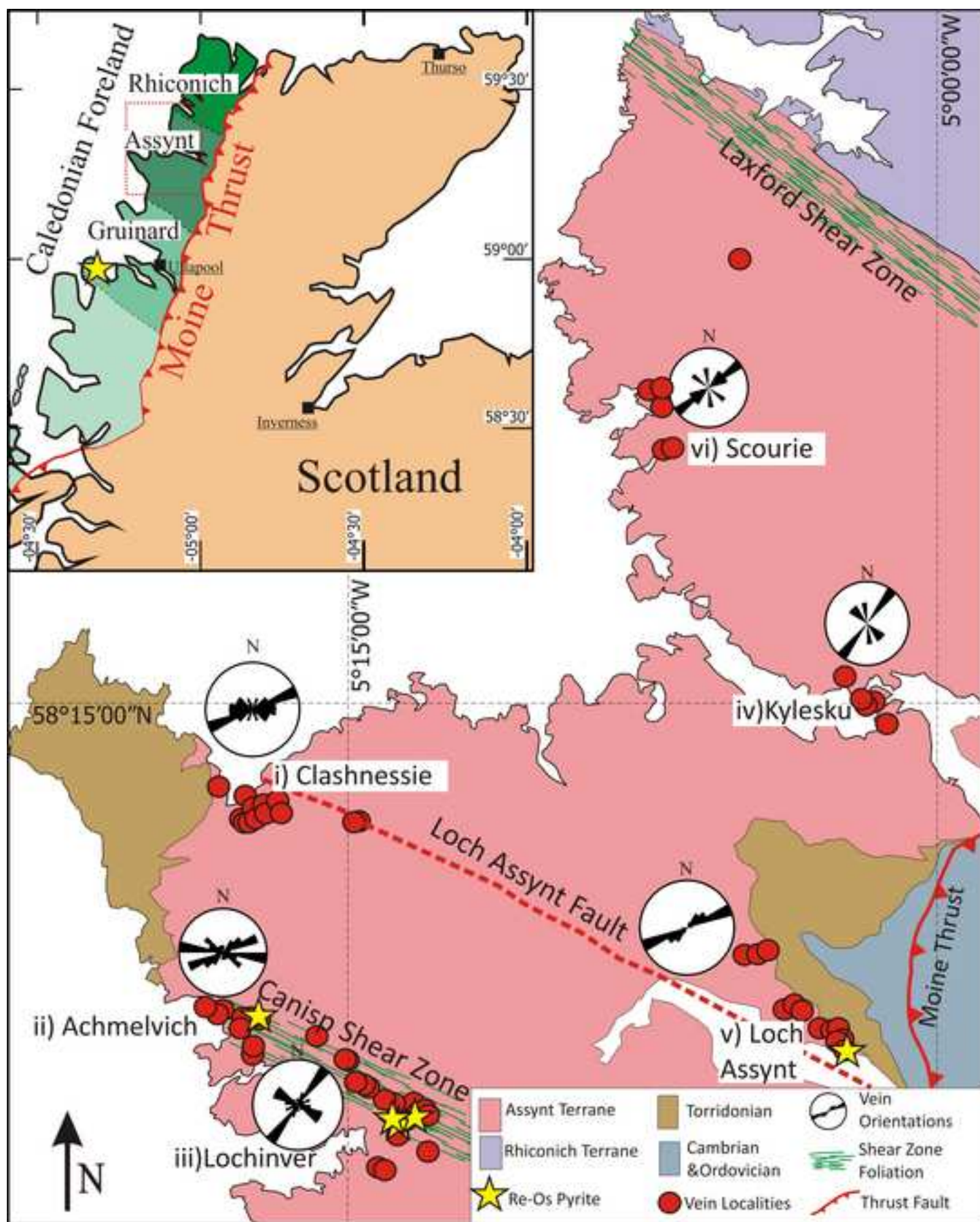
Formatted: Superscript

Table 1: Re-Os and S isotope data for pyrite from quartz veins in the Lewisian Complex, NW Scotland.

Batch/Sample	Location (Lat/Long) / OS	Re (ppb) total	±	Os (ppt) total	±	¹⁸⁷ Re/ ¹⁸⁸ Os	±	¹⁸⁷ Os/ ¹⁸⁸ Os	±	rho	¹⁸⁷ Re (ppb)	±	¹⁸⁷ Os ^f (ppt) ¹	±	¹⁸⁷ Os ^f (ppt) ²	±	% ¹⁸⁷ Os ^f	Model age ³	±	Model age ⁴	±	d ³⁴ S (‰) ⁵
<i>Gcinard Bay</i>																						
RO297-2/G-Bay	57°51.567' N / 005° 27.121' W 8310, 7817	25.2	0.1	602.1	45.1	12670.5	627.9	473.6	27.4	0.851	15.86	0.06	591.6	21.1	589.0	24.1	99.8	2198.5	78.9	2189.0	90.1	3.0
<i>Lochan Sgeireach</i>																						
RO297-3/28	58°10.640' N / 005°16.374'W 0755, 2560	6.8	0.0	298.8	26.9	265.6	21.2	11.04	1.4	0.636	4.27	0.02	163.1	145.7	129.3	209.8	91.8 - 72.8	2249.4	2010.2	1790.5	2904.7	1.1
<i>Waterworks</i>																						
RO297.5/64.1	58°09.049' N / 005°13.357' W 1038, 2249	8.0	0.0	242.8	33.9	395.1	49.5	11.56	2.2	0.663	5.02	0.02	135.5	116.3			92.2	1597.6	1371.2			-2.2
<i>Lochniver</i>																						
RO143-1/BH2	58°09.599' N / 005°13.530'W	25.8	0.1	660.5	23.3	4762.4	123.4	186.3	4.9	0.963	16.22	0.06	631.7	30.9	624.6	44.4	99.5	2293.0	112.5	2267.5	161.6	1.9
RO143-4/BH5	58°09.599' N / 005°13.530'W 1012, 2366	23.8	0.1	623.8	20.0	4041.8	96.9	160.8	3.8	0.974	14.98	0.06	592.5	33.4	584.7	48.2	99.4	2328.7	131.7	2298.7	189.8	1.8
<i>Loch Assynt</i>																						
RO194-2/LA2	58°10.703' N / 005°02.471' W 2050, 2540	14.6	0.1	358.2	49.4	17531.0	1729.3	675.2	66.6	0.998	9.19	0.04	353.8	5.0	352.7	7.0	99.8	2265.5	32.9	2258.6	45.7	0.9

Figure

[Click here to download high resolution image](#)



Figure

[Click here to download high resolution image](#)

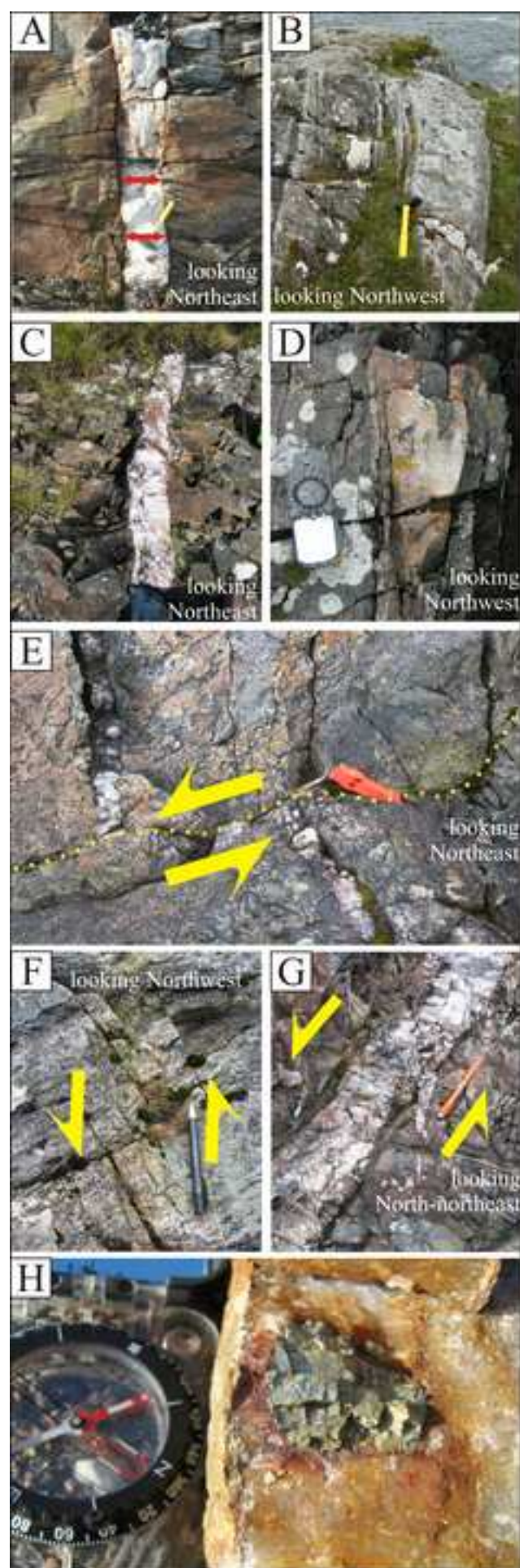
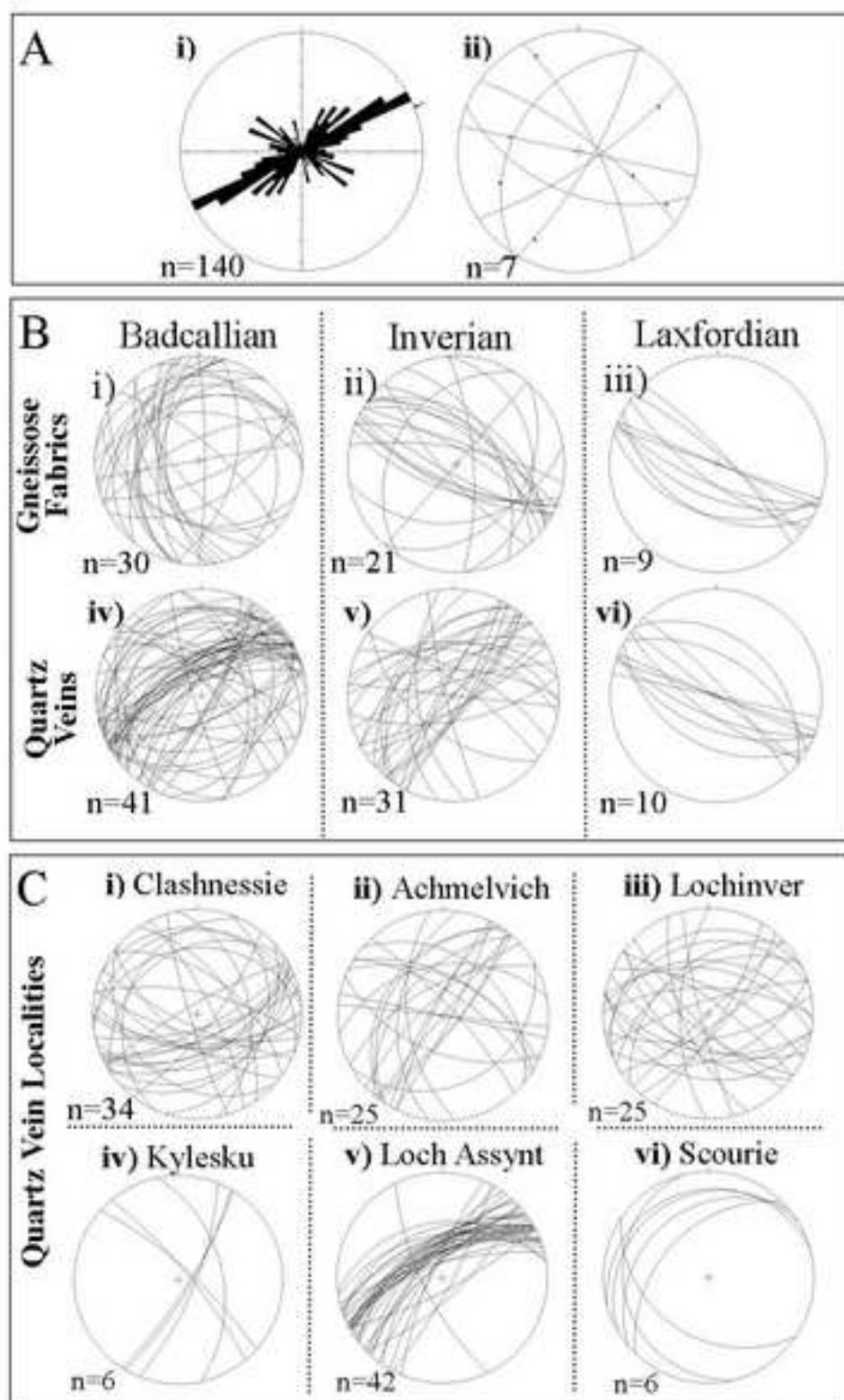
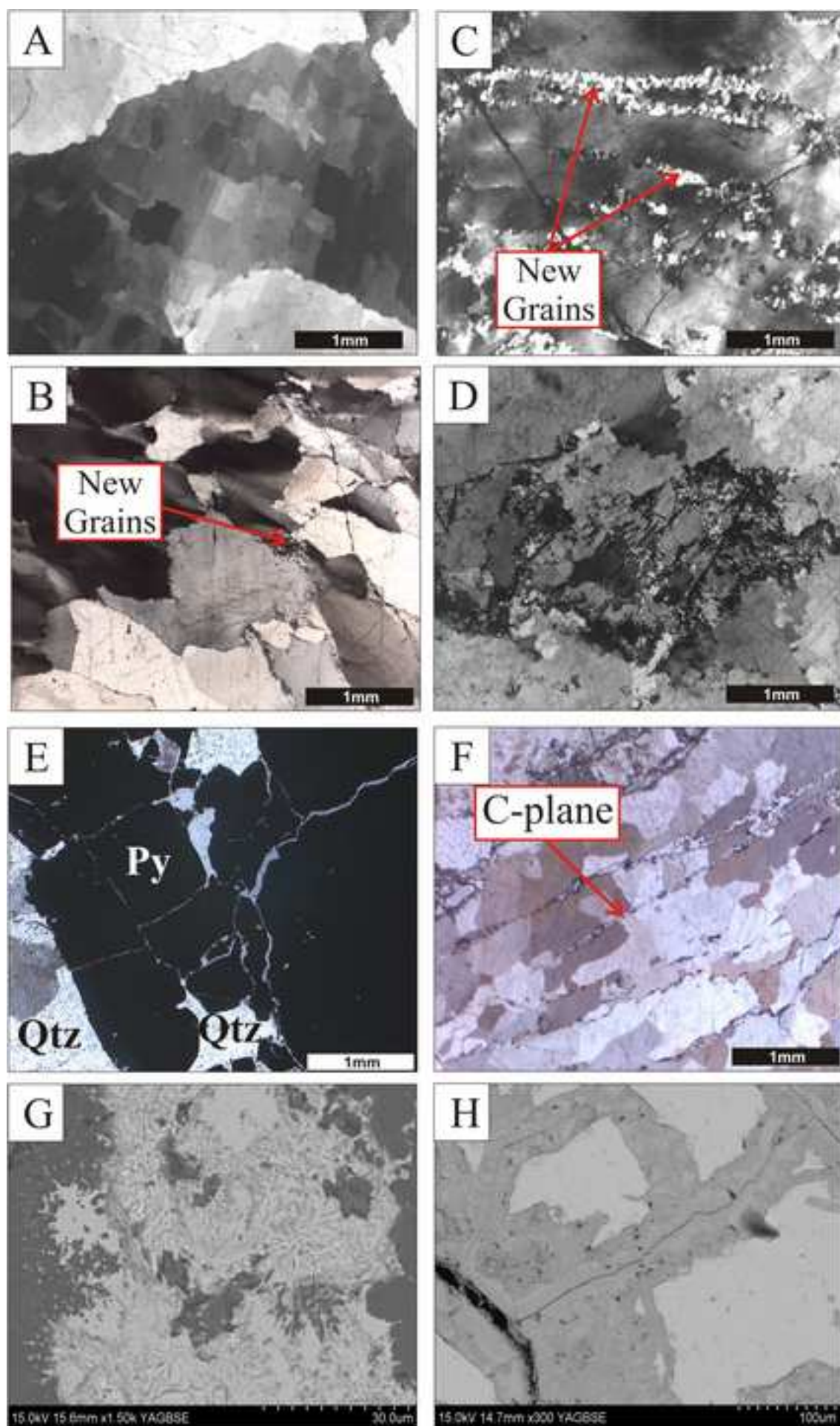


Figure
[Click here to download high resolution image](#)



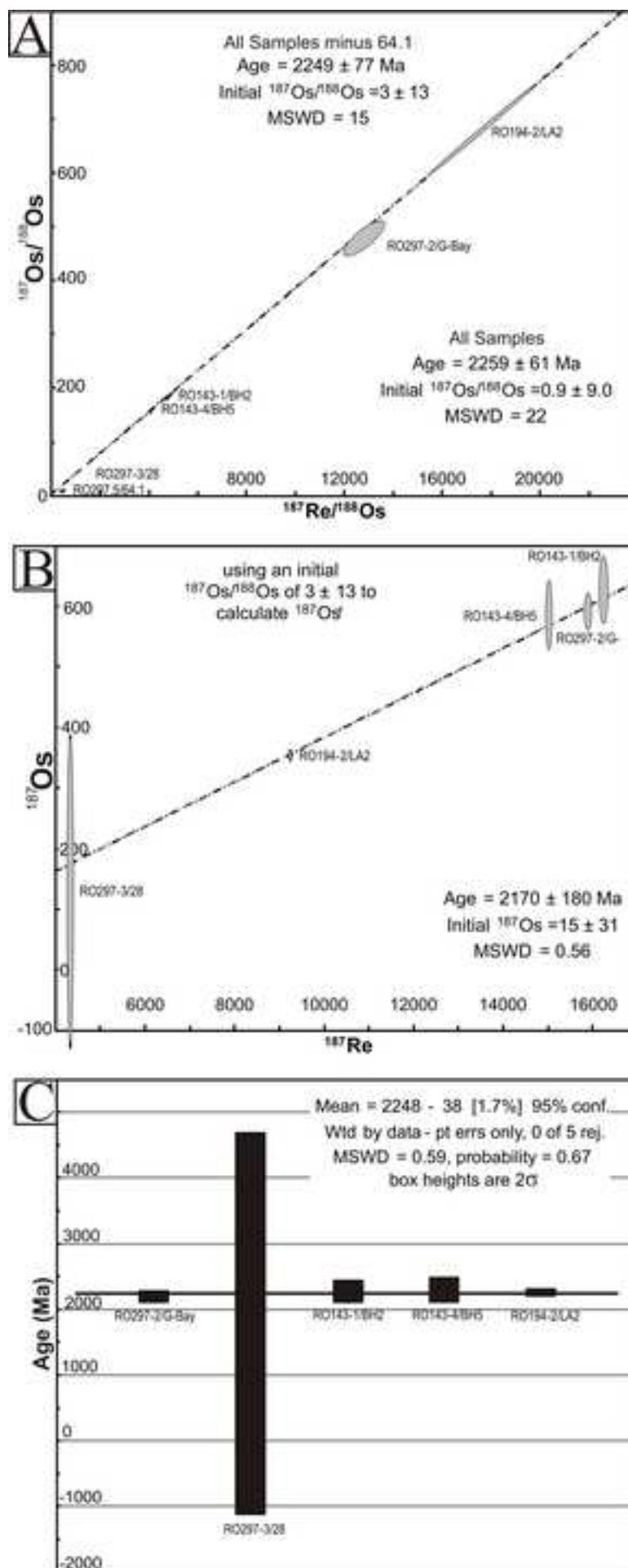
Figure

[Click here to download high resolution image](#)



Figure

[Click here to download high resolution image](#)



Figure

[Click here to download high resolution image](#)

